

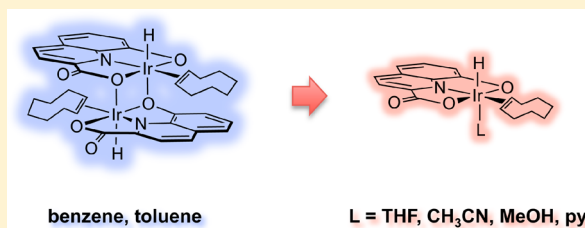
Unsaturated Iridium(III) Complexes Supported by a Quinolato–Carboxylato ONO Pincer-Type Ligand: Synthesis, Reactivity, and Catalytic C–H Functionalization

Duc Hanh Nguyen, Jesús J. Pérez-Torrente,* M. Victoria Jiménez, F. Javier Modrego, Daniel Gómez-Bautista, Fernando J. Lahoz, and Luis A. Oro*

Departamento de Química Inorgánica, Instituto de Síntesis Química y Catálisis Homogénea-ISQCH, Facultad de Ciencias, Universidad de Zaragoza-CSIC, C/Pedro Cerbuna, 12, 50009 Zaragoza, Spain

S Supporting Information

ABSTRACT: The unsaturated σ,π -cyclooctenyl iridium(III) pincer compound $[\text{Ir}(\kappa^3\text{-hqca})(1\text{-}\kappa\text{-}4,5\text{-}\eta\text{-}\text{C}_8\text{H}_{13})]$ (**1**) has been prepared by the reaction of $[\text{Ir}(\text{cod})(\text{CH}_3\text{CN})_2]\text{BF}_4$ with lithium 8-oxidoquinoline-2-carboxylate (Li_2hqca) and obtained as two isomers derived from the relative disposition of the pincer and the σ,π -cyclooctenyl ligands. Compound **1** can be prepared as a single isomer by reaction of 8-hydroxyquinoline-2-carboxylic acid (H_2hqca) with $[\text{Ir}(\mu\text{-OMe})(\text{cod})]_2$. Reaction of $[\text{Ir}(\mu\text{-OH})(\text{coe})_2]_2$ with H_2hqca gave the square-pyramidal iridium(III) complex $[\text{IrH}(\kappa^3\text{-hqca})(\text{coe})]$ (**3**). This compound exists as dinuclear assemblies $[\text{IrH}(\kappa^3\text{-hqca})(\text{coe})]_2$ in noncoordinating solvents and as the corresponding labile mononuclear solvates in more polar solvent solutions. The dimerization of **3** was established by ^1H -DOSY NMR spectroscopy and an ESI^+ mass spectrum and supported by DFT calculations. Reaction of **3** with pyridine gave the adduct $[\text{IrH}(\kappa^3\text{-hqca})(\text{coe})(\text{py})]$ (**4**) and the bis-pyridine complexes $[\text{IrH}(\kappa^3\text{-hqca})(\text{R-py})_2]$ ($\text{R} = \text{H}$ (**6**), 2-Me (**7**)) by replacement of the coe ligand. Compound **4** was transformed into the bromo derivative $[\text{IrBr}(\kappa^3\text{-hqca})(\text{coe})(\text{py})]$ (**5**) by reaction with *N*-bromosuccinimide. Carbonylation of **4** gave the cyclooctenyl complex $[\text{Ir}(\kappa^3\text{-hqca})(1\text{-}\kappa\text{-}\text{C}_8\text{H}_{15})(\text{CO})(\text{py})]$ (**8**), which is stable only under a carbon monoxide atmosphere. The pincer complexes were active in the catalytic borylation of arenes under thermal conditions.



INTRODUCTION

Pincer ligands capable of coordinating to the metal center in a meridional tridentate configuration are ubiquitous in recent organometallic chemistry.¹ In spite of the apparent simplicity of the ligand framework, pincer ligands are valuable structural motifs for the design of transition-metal complexes for selective stoichiometric and catalytic transformations.² In fact, pincer complexes were found to efficiently catalyze a variety of reactions, including hydrogenation,³ dehydrogenation based on C–H bond activation processes,⁴ coupling reactions,⁵ and related processes.⁶ In general, the tridentate coordination mode, which results in the formation of two five-membered chelate rings, confers an outstanding thermal stability to metal complexes that allows them to operate even under harsh conditions.^{4,7} Pincer ligands having O-donor fragments have been much less studied than those bearing C-, N-, P-, or S-donor-based functionalities.⁸ In this context, the ability of OCO and ONO trianionic pincer ligands for supporting high-oxidation-state metal complexes with vacant coordination sites, which has been recently exploited for a range of catalytic transformations, is remarkable.^{9,10}

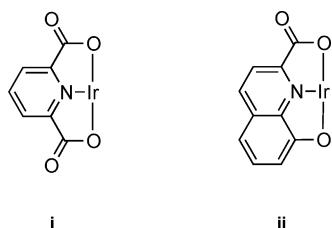
On the other hand, the development of selective metal-mediated C–H bond functionalization processes is still a challenge because of its potentially large applicability to organic

synthesis.¹¹ Low-valent iridium complexes have been reported to show good activity for C–H activation and functionalization processes.¹² Recently, O-based dianionic pincer ligands have attracted considerable attention regarding the iridium-mediated activation of C–H bonds.¹³ The robustness and stability of the ligand framework, with strongly electron donating hard oxygen donor atoms, can provide more facile access to the relatively high oxidation state of the metal center, thereby promoting the C–H bond oxidative addition under mild conditions.¹⁴ We have reported the synthesis of iridium(III) pyridinedicarboxylate pincer complexes (Chart 1(i)) which exhibited a notable catalytic activity in borylation of aromatic compounds involving C–H bond activation under thermal conditions.¹⁵ These complexes were straightforwardly prepared from several pyridine-2,6-dicarboxylic acids and standard dinuclear iridium(I) complexes $[\text{Ir}(\mu\text{-OR})(\text{cod})]_2$ ($\text{R} = \text{Me}, \text{H}$). The application of this synthetic methodology to other dicarboxylic acid precursors for dianionic tridentate pincer ONO complexes has so far shown a narrow scope. However, the reactivity studies on some iminodiacetic acid derivatives, $\text{RN}(\text{CH}_2\text{COOH})_2$ ($\text{R} = \text{Me}, \text{Ph}$), has allowed us to identify the

Received: August 1, 2013

Published: November 8, 2013

Chart 1. Ligand Framework of ONO-Based Dianionic Pincer Iridium Complexes



acidity (pK_a) and the rigidity of the potential tridentate ligand precursor as the key factors leading to the preparation of iridium(III) complexes.¹⁶

In order to test whether this synthetic method could be applied to the direct synthesis of related dianionic tridentate pincer ONO iridium(III) complexes, we have explored the reactivity of 8-hydroxyquinoline-2-carboxylic acid.¹⁷ This asymmetrical flat ONO pincer ligand precursor is more rigid than the symmetric pyridinedicarboxylate species due to the presence of the quinolinol moiety (Chart 1(ii)). Taking as a reference the acid dissociation constants of 8-hydroxyquinoline ($pK_a = 9.89$)¹⁸ and quinoline-2-carboxylic acid ($pK_a = 1.45$),¹⁹ it also became evident that 8-hydroxyquinoline-2-carboxylic acid is less acidic than 2,6-pyridinedicarboxylic acid ($pK_a = 2.10$ and 4.38).²⁰ We report herein on the synthesis and reactivity of unsaturated iridium(III) complexes supported by the asymmetrical dianionic ONO pincer-type ligand 8-oxidoquinoline-2-carboxylate. In addition, the study of an unusual solvent-dependent dimerization reaction and its application in the catalytic C–H borylation of arenes is also reported.

RESULTS AND DISCUSSION

Synthesis and Reactivity of $[\text{Ir}(\kappa^3\text{-hqca})(1\text{-}\kappa\text{-}4,5\text{-}\eta\text{-}\text{C}_8\text{H}_{13})](\text{MeOH})$. The reaction of 8-hydroxyquinoline-2-carboxylic acid (H_2hqca) with 0.5 molar equiv of the dinuclear iridium methoxy-bridged complex $[\text{Ir}(\mu\text{-OMe})(\text{cod})]_2$, in a $\text{CH}_2\text{Cl}_2/\text{MeOH}$ solution at room temperature, gave a dark red solution of the complex $[\text{Ir}(\kappa^3\text{-hqca})(1\text{-}\kappa\text{-}4,5\text{-}\eta\text{-}\text{C}_8\text{H}_{13})]$ (**1**), which was isolated in 88% yield as a red microcrystalline solid after chromatographic purification. Compound **1** is barely soluble in most organic solvents, including dichloromethane or methanol, although it has an acceptable solubility in a 5:1 mixture of both solvents. The compound has been fully characterized by NMR spectroscopy and by a single-crystal X-ray diffraction study of the methanol solvate, **1**·MeOH, which confirmed the presence of the pincer 8-oxidoquinoline-2-carboxylate ligand and a σ,π -cyclooctenyl ligand coordinated in a $1\text{-}\kappa\text{-}4,5\text{-}\eta$ fashion (Figure 1). The coordination geometry around the iridium(III) center is distorted octahedral, in which the rigid doubly deprotonated flat ONO tridentate ligand occupies a meridional position with the double bond of the σ,π -cyclooctenyl ligand *trans* to the quinoline nitrogen, and a methanol molecule is linked *trans* to the alkylic Ir–C bond. Major distortions from the octahedral environment arise from the chelating units within the tridentate *hqca* group (mean O–Ir–N = $78.75(8)^\circ$) and, in a minor extension, from the chelating nature of the σ,π -bonded cyclooctenyl ligand (C(11)–Ir–M = $78.12(14)^\circ$; see Figure 1). The olefin exhibits a slightly twisted conformation with regard to the *hqca* plane (dihedral angle *hqca* vs Ir–olefin plane, $45.3(2)^\circ$).

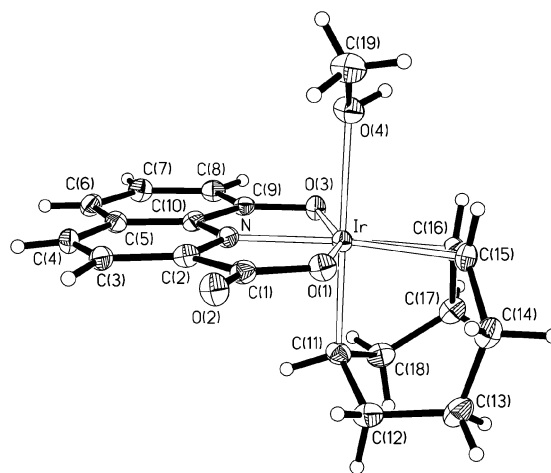


Figure 1. Molecular structure of $[\text{Ir}(\kappa^3\text{-hqca})(1\text{-}\kappa\text{-}4,5\text{-}\eta\text{-}\text{C}_8\text{H}_{13})](\text{MeOH})$ (**1**·MeOH). Selected bond distances (Å) and angles (deg): Ir–O(1) = 2.090(2), Ir–O(3) = 2.092(2), Ir–O(4) = 2.275(3), Ir–N = 1.974(3), Ir–C(11) = 2.056(4), Ir–C(15) = 2.168(4), Ir–C(16) = 2.168(3), C(15)–C(16) = 1.401(5); O(1)–Ir–O(3) = $157.05(10)$, O(1)–Ir–O(4) = $90.30(10)$, O(1)–Ir–N = $77.34(11)$, O(1)–Ir–C(11) = $93.87(13)$, O(1)–Ir–M = $102.77(13)$, O(3)–Ir–O(4) = $85.28(10)$, O(3)–Ir–N = $80.15(11)$, O(3)–Ir–C(11) = $90.99(13)$, O(3)–Ir–M = $99.99(14)$, O(4)–Ir–N = $90.04(11)$, O(4)–Ir–C(11) = $175.81(11)$, O(4)–Ir–M = $93.95(13)$, N–Ir–C(11) = $91.19(14)$, N–Ir–M = $176.00(14)$, C(11)–Ir–M = $78.12(14)$. M represents the midpoint of the olefinic C(15)–C(16) double bond.

The whole molecule resembles quite well the analogous complex $[\text{Ir}(\kappa^3\text{-pydc})(1\text{-}\kappa\text{-}4,5\text{-}\eta\text{-}\text{C}_8\text{H}_{13})](\text{MeOH})$ containing the 2,6-pyridinedicarboxylate as tridentate pincer ligand.¹⁵ As observed in the pyridinedicarboxylate analogue, the Ir–O(1) and Ir–O(3) bond distances in **1**, 2.090(2) and 2.092(2) Å, respectively, are remarkably shorter than the Ir–O(4) bond distance of the coordinated methanol ligand, 2.275(3) Å, which reflects the high structural *trans* influence of the alkylic Ir–C bond. The apparent greater rigidity of the quinoline derivative in comparison to that of the *pydc* analogue has no effect on the relative disposition of both *trans* oxygens, giving rise to identical O(1)–Ir–O(3) bond angles in both complexes, $157.31(11)$ vs $157.05(10)^\circ$ in **1**.

Although two isomers derived from the relative disposition of the pincer ligand with respect to the σ,π -cyclooctenyl ligand could be expected (**1a,b**; Figure 2), NMR spectroscopic data

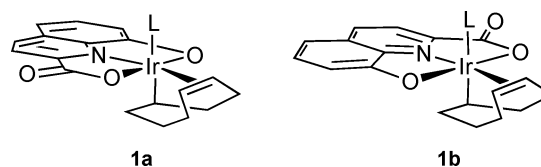


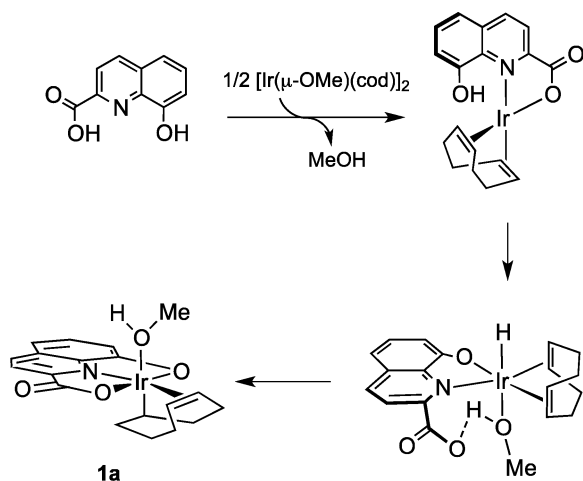
Figure 2. Isomers of $[\text{Ir}(\kappa^3\text{-hqca})(1\text{-}\kappa\text{-}4,5\text{-}\eta\text{-}\text{C}_8\text{H}_{13})]$ (**1**; L = MeOH).

and the structure determination confirmed the exclusive formation of the isomer **1a**. In a complementary synthetic approach, reaction of the cationic mononuclear complex $[\text{Ir}(\text{cod})(\text{CH}_3\text{CN})_2]\text{BF}_4$ with lithium 8-oxidoquinoline-2-carboxylate (Li_2hqca) in $\text{CH}_2\text{Cl}_2/\text{MeOH}$ also gave **1** in 92% yield. However, the ^1H NMR spectrum evidenced the formation of a 1:1 diastereoisomer mixture of **1a** and **1b**. Most probably the adventitious water in the organic solvents is the proton source

for the formation of the cyclooctenyl ligand. In fact, when the reaction was carried out in the presence of added water, compound **1** was also obtained as an isomer mixture in which **1a** predominates (70%). The ^1H NMR spectrum of **1a** in $\text{CD}_3\text{OD}/\text{CD}_2\text{Cl}_2$ showed five resonances between 8.2 and 6.8 ppm for the 8-oxidoquinoline-2-carboxylato ligand and a set of resonances for the cyclooctenyl ligand. Full assignment of the resonances and connectivity for both groups of resonances was achieved with the help of two-dimensional NMR techniques (see the Experimental Section). The olefinic protons ($=\text{CH}$) were observed as two low-field multiplet resonances at 5.73 and 5.54 ppm which correlated with those at 87.80 and 82.98 ppm in the $^{13}\text{C}\{^1\text{H}\}$ NMR spectrum. The Ir–CH resonance (C-1) was observed at 13.19 ppm. Isomer **1b** showed an identical, slightly shifted set of resonances for both types of ligands.

A feasible mechanism for the stereoselective formation of **1a** is shown in Scheme 1. Taking into account that, in general,

Scheme 1. Proposed Mechanism for the Selective Formation of $[\text{Ir}(\kappa^3\text{-hqca})(1\text{-}\kappa\text{-}4,5\text{-}\eta\text{-}\text{C}_8\text{H}_{13})]$ (1a**; L = MeOH)**



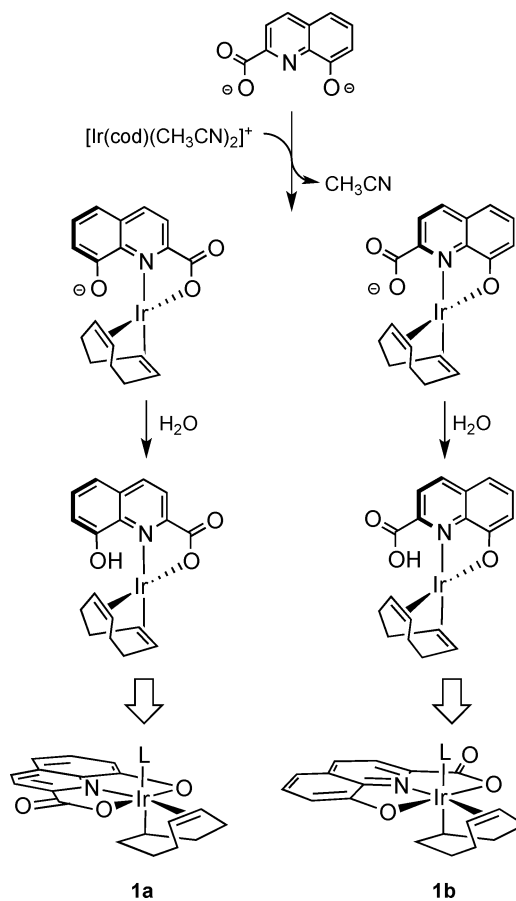
carboxylic acids are more acidic than phenol derivatives, it is reasonable to propose the selective protonation of the methoxido bridges in $[\text{Ir}(\mu\text{-OMe})(\text{cod})]_2$ by the acidic carboxyl group of H_2hqca to give the mononuclear neutral iridium(I) intermediate $[\text{Ir}(\kappa^2\text{-Hhqca})(\text{cod})]$ having the monodeprotonated ligand $\kappa^2\text{-N,O}$ coordinated through the carboxylate moiety. By analogy with the mechanism operating in the formation of the related pyridine-2,6-dicarboxylate complex,¹⁶ the formation of **1a** involves a metal-mediated proton transfer to the 1,5-cyclooctadiene ligand through the methanol-stabilized hydrido species $[\text{IrH}(\kappa^2\text{-hqca})(\text{cod})(\text{CH}_3\text{OH})]$, featuring a hydrogen bond with the uncoordinated carboxylate moiety of the 8-oxidoquinoline-2-carboxylato ligand $\kappa^2\text{-N,O}$ coordinated. Most probably, the formation of this key hydrido intermediate also results from solvent-assisted proton transfer through a hydrogen-bonding network instead of the less favorable direct protonation of the iridium center by the phenol moiety, formally an oxidative addition.²¹ Hydride migration to the double bond of the cod ligand *trans* to the O-donor atom keeping the remaining double bond *trans* to quinoline should result in the formation of the σ,π -cyclooctenyl complex with the required stereochemistry (**1a**).

Unfortunately, monitoring of the reaction by ^1H NMR at low temperature did not allow for the characterization of any intermediates, as only featureless resonances were observed

from the beginning of the reaction. However, the full characterization of the deuterium labeled compound **1-d₁** supports the hydrido route against a potential intermolecular direct protonation of the cyclooctadiene ligand. Thus, reaction of $[\text{Ir}(\text{cod})(\text{CH}_3\text{CN})_2]^+$ with Li_2hqca in the presence of D_2O gave the expected isomer mixture of **1** with deuterium incorporation in both isomers. The $^{13}\text{C}\{^1\text{H}\}$ NMR spectrum showed two deuterium-coupled triplet resonances for the C-8 resonance of the $\text{C}_8\text{H}_{12}\text{D}$ cyclooctenyl ligand of both isomers at 33.64 ($J_{\text{D-C}} = 20.6$ Hz, **1a-d₁**) and 33.50 ppm ($J_{\text{D-C}} = 20.6$ Hz, **1b-d₁**). Furthermore, the lack of the resonances attributable to the 8-H-*endo* protons in the ^1H NMR spectrum (1.04 ppm for **1a**) supports the hydrido/insertion mechanism depicted in Scheme 1, as the migratory insertion proceeds with *cis* stereochemistry.

The two parallel reaction pathways outlined in Scheme 2 provided a rational explanation for the formation of the isomer

Scheme 2. Reaction Pathways Leading to an Isomer Mixture of $[\text{Ir}(\kappa^3\text{-hqca})(1\text{-}\kappa\text{-}4,5\text{-}\eta\text{-}\text{C}_8\text{H}_{13})]$ (1**; L = MeOH)**



mixture of **1** starting from the lithium 8-oxidoquinoline-2-carboxylate salt (Li_2hqca). Replacement of the labile acetonitrile ligands in $[\text{Ir}(\text{cod})(\text{CH}_3\text{CN})_2]^+$ by Li_2hqca gives two mononuclear anionic iridium(I) intermediates $[\text{Ir}(\kappa^2\text{-hqca})(\text{cod})]^-$ having the tridentate ligand $\kappa^2\text{-N,O}$ coordinated through the carboxylate and phenolate moieties, respectively. Then, reaction with water would result in the protonation of the uncoordinated functions, giving the corresponding phenol and carboxyl neutral complexes $[\text{Ir}(\kappa^2\text{-Hhqca})(\text{cod})]$, respectively. Solvent-assisted proton transfer to the iridium center in both intermediates followed by olefin insertion gives isomers

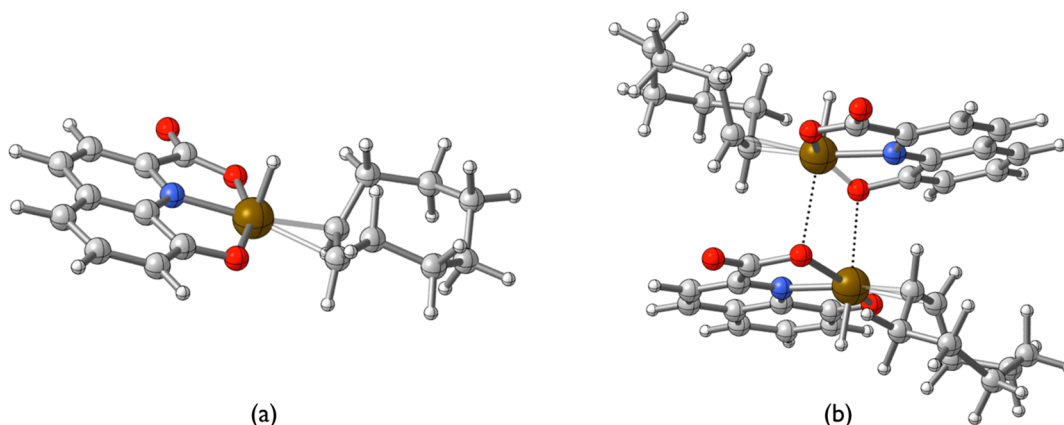


Figure 3. DFT geometry-optimized structures of (a) $[\text{IrH}(\kappa^3\text{-hqca})(\text{coe})]$ (**3**) and (b) the mixed dinuclear assembly $[\text{IrH}(\kappa^3\text{-hqca})(\text{coe})]_2$.

1a,b, respectively, through the corresponding iridium(III) hydrido intermediates.

Reaction of **1a** in refluxing pyridine gave $[\text{Ir}(\kappa^3\text{-hqca})(1\text{-}\kappa\text{-4,5-}\eta\text{-C}_8\text{H}_{13})(\text{py})]$ (**2a**), which was isolated as a red solid in excellent yield. As could be expected, when an isomer mixture of **1** (**1a,b**, 70% of **1a**) was reacted with pyridine under the same conditions compound **2** was isolated as an isomer mixture, **2a,b** (74% of **2a**), in similar yield. Both isomers of **2** have been fully characterized by NMR spectroscopy and showed the expected sets of resonances for the 8-oxidoquinoline-2-carboxylato, σ,π -cyclooctenyl, and pyridine ligands at very close chemical shifts. Compound **2** is labile, as a consequence of the *trans* effect exerted by the alkyl bond, and undergoes fast pyridine exchange with $\text{py-}d_5$ (*) at room temperature. Monitoring of a CD_2Cl_2 solution of **2** (0.023 M) after addition of a 5-fold excess of $\text{py-}d_5$ showed that the equilibrium between **2a** and **2a*** ($K \approx 0.2$) was reached in less than 5 min.

Synthesis and Dimerization of $[\text{IrH}(\kappa^3\text{-hqca})(\text{coe})]$.

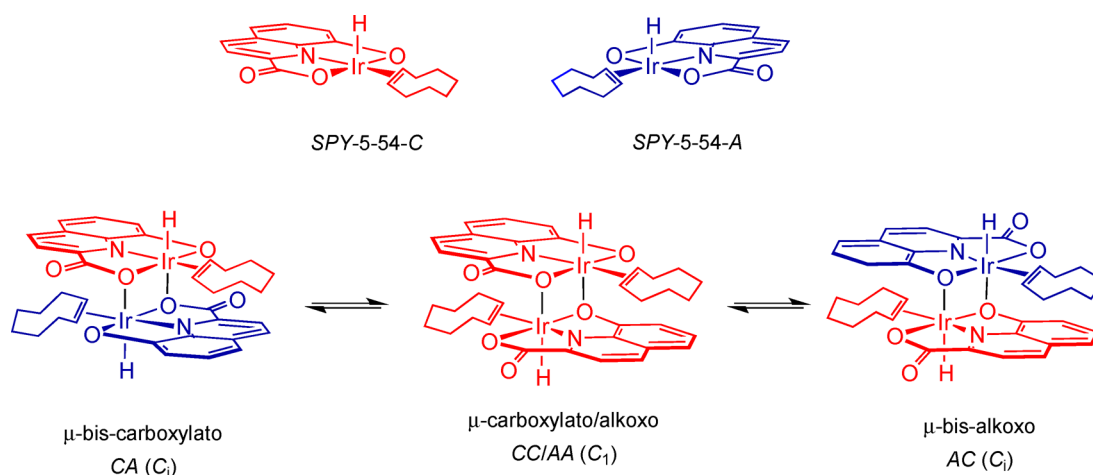
Reaction of the dinuclear cyclooctene iridium hydroxy-bridged $[\text{Ir}(\mu\text{-OH})(\text{coe})_2]$ complex with 2 equiv of 8-hydroxyquinoline-2-carboxylic acid gave a dark red solution of the compound $[\text{IrH}(\kappa^3\text{-hqca})(\text{coe})]$ (**3**), which was isolated as a red solid in quantitative yield. The analytical and spectroscopic data for **3** suggest an unsaturated square-pyramidal iridium(III) complex having the hydrido ligand at the apical position. In fact, the ^1H NMR spectrum of **3** in $\text{THF-}d_8$ showed, apart from the expected set of resonances for the tridentate 8-oxidoquinoline-2-carboxylato and cyclooctene ligands, a resonance shifted strongly upfield at -36.26 ppm, which is typical of hydrido complexes with a vacant site in a *trans* position.²² Interestingly, the addition of methanol- d_4 resulted in a decrease of the intensity of the hydrido resonance due to fast H/D exchange. The exchange process was also confirmed in the ^2H NMR spectrum of **3-}d_1, which showed a singlet resonance at -34.72 ppm.**

The ^1H NMR spectrum of **3** in C_6D_6 is puzzling, since it exhibits four high-field resonances of the same intensity at -33.54 , -34.03 , -34.38 , and -35.98 ppm, the last signal being somewhat broad (see below). The ESI^+ mass spectrum in toluene showed two peaks corresponding to the dinuclear species $[\text{3}_2] + \text{Na}^+$ and $[\text{3}_2] + \text{H}^+$ at m/z 1003.2 and 981.2, respectively, which points to the presence of dinuclear species $[\text{IrH}(\kappa^3\text{-hqca})(\text{coe})]_2$ in solution. In sharp contrast, the FAB mass spectrum in THF did not show any evidence for the presence of dinuclear species.

The DFT geometry-optimized structure of the mononuclear complex $[\text{IrH}(\kappa^3\text{-hqca})(\text{coe})]$ (**3**) is shown in Figure 3a. The iridium atom shows an almost ideal square-pyramidal coordination with the hydrido ligand at the vertex of the pyramid with an Ir–H distance of 1.53 Å. At the basal plane the tridentate ligand spans an angle O–Ir–O of 157.5° with the Ir–N vector almost bisecting it ($\text{O}_{\text{ph}}\text{–Ir–N} = 79.7^\circ$, $\text{O}_{\text{cx}}\text{–Ir–N} = 78.3^\circ$). The assembly of two square-pyramidal (*SPY-5-54*)²³ could take place through both the carboxylate and phenolate moieties of the tridentate ligand, resulting in two octahedral iridium(III) centers bridged by two 8-oxidoquinoline-2-carboxylato ligands, exhibiting a $1\kappa\text{O}, 1\kappa\text{N}, 1:2\kappa^2\text{O}$ coordination mode, forming a central four-membered Ir_2O_2 ring. Figure 3b shows the DFT geometry-optimized structure of the mixed dinuclear assembly through carboxylate and phenolate moieties. The coordination environment of the iridium atoms becomes octahedral after dimerization, with the *exo* molecular oxygen donor atoms occupying the sixth, formerly vacant, coordination position, which is empty in the square-pyramidal monomer. The coordination is weak, as is shown by the long Ir–O distances ($\text{Ir–O}'_{\text{cx}} = 2.58$ Å, $\text{Ir–O}'_{\text{ph}} = 2.50$ Å). Both the carboxylate and phenoxide groups are tilted toward the respective iridium atom to which they are coordinated, leading to the dihedral angles $\text{Ir–N–C}_{\text{cx}}\text{–O}_{\text{cx}} = 12.8^\circ$ and $\text{Ir–N–C}_{\text{ph}}\text{–O}_{\text{ph}} = 15.9^\circ$. Gas-phase calculations show a dimerization energy of $\Delta E = -12.66$ kcal/mol, but a calculated ΔG of $+4.9$ kcal/mol results because of the known penalty favoring dissociation of the gas phase, which is due to an overestimation of the entropy factor.²⁴

The existence of dinuclear assemblies in nonpolar solvents, or weakly coordinating solvents such as CH_2Cl_2 , was further corroborated by means of ^1H -DOSY NMR spectroscopy.²⁵ The resonances of the aromatic protons of the 8-oxidoquinoline-2-carboxylato ligand (**3** in tetrahydrofuran- d_8) or the hydrido resonances (**3** in benzene- d_6) were used for the determination of the diffusion coefficients (*D*) at 300 K. As expected, the *D* value measured in tetrahydrofuran- d_8 , $8.44 \times 10^{-10} \text{ m}^2 \text{ s}^{-1}$, is larger than that in benzene- d_6 , $5.33 \times 10^{-10} \text{ m}^2 \text{ s}^{-1}$, which is in agreement with the fact that larger structures should have smaller diffusion coefficients because they move more slowly. Interestingly, the *D* values obtained from the four different hydrido resonances of the dinuclear assemblies in benzene- d_6 were very similar, in the range $(5.25\text{--}5.36) \times 10^{-10} \text{ m}^2 \text{ s}^{-1}$, which excludes the presence of mononuclear **3** in an appreciable concentration. From these data the hydrodynamic radii (r_{H}) were calculated by applying a modified Stokes–Einstein

Scheme 3. Dinuclear Assemblies Observed in the Dimerization of the Square-Pyramidal Chiral Complex $[\text{IrH}(\kappa^3\text{-hqca})(\text{coe})]$ (3)



equation.²⁶ The determined r_{H} values for $[\mathbf{3}]_2$ and $\mathbf{3}\cdot\text{THF}$ were 7.17 and 5.94 Å, respectively. The radii calculated with the volumes determined from the optimized geometries were: $r_{\text{H}}([\mathbf{3}]_2) = 6.78$ Å, $r_{\text{H}}(\mathbf{3}) = 5.51$ Å, and $r_{\text{H}}(\mathbf{3}\cdot\text{THF}) = 5.87$ Å (see the Supporting Information). The radius ratio determined from the calculated radii, $r_{\text{H}}([\mathbf{3}]_2)/r_{\text{H}}(\mathbf{3}\cdot\text{THF})$, of 1.15 deviates somehow from the ratio of 1.20 determined experimentally. However, much better agreement was attained when this value was compared with the radius ratio $r_{\text{H}}([\mathbf{3}]_2)/r_{\text{H}}(\mathbf{3})$ of 1.23. Thus, even considering the experimental uncertainty, these data point to a very weak interaction of THF with $\mathbf{3}$.

The successful interpretation of the ^1H NMR spectrum in C_6D_6 requires considering the stereochemistry of the potential dinuclear assemblies. The mononuclear complex $\mathbf{3}$ is chiral and exists as two enantiomers, *SPY-5-54-C* and *SPY-5-54-A*, the existence of several stereoisomers being possible. Dinuclear entities with both *cis* and *trans* relative dispositions of the tridentate ligands could be assembled depending on the chirality of the mononuclear components. Nevertheless, molecular models have shown that the *trans* assemblies are strongly favored from a steric point of view, as the repulsion between the cyclooctene ligands is avoided. Taking the above into consideration, four stereoisomeric assemblies could be expected (Scheme 3).²⁷ The assembly involving both carboxylate or phenolate moieties requires mononuclear components with opposite chirality (*A* and *C*) and results in the formation of dinuclear complexes (*CA*) with C_i symmetry having equivalent hydrido ligands. In contrast, the assembly of square-pyramidal complexes of the same chirality requires carboxylate and phenolate bridging ligands and gives an enantiomeric pair (*AA* and *CC*), indistinguishable by NMR, having nonequivalent hydrido ligands.

This interpretation accounts for the number and intensity of the hydrido resonances in the ^1H NMR (C_6D_6) spectrum and also for the chemical inequivalence of the two $=\text{CH}$ protons of each *coe* ligand. Furthermore, the stereoisomers interconvert in solution, as evidenced by the cross-peaks observed in the ^1H – ^1H NOESY spectrum, in both the hydride (Figure 4) and olefinic regions. Thus, the four stereoisomers take part in a dynamic equilibrium involving the exchange of square-pyramidal components, which confirms the weak interaction between the mononuclear components into the dinuclear assemblies. In fact, the addition of methanol or acetonitrile to

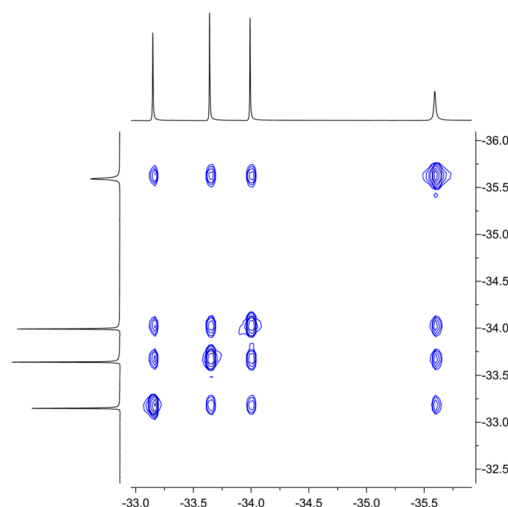


Figure 4. High-field region of the ^1H – ^1H NOESY spectrum of $[\text{IrH}(\kappa^3\text{-hqca})(\text{coe})]$ ($\mathbf{3}$) in C_6D_6 at 298 K.

solutions of $\mathbf{3}$ in C_6D_6 or toluene- d_8 resulted in the formation of mononuclear hydrido complexes that have been characterized as the solvato $\mathbf{3}\cdot\text{MeOH}$ and $\mathbf{3}\cdot\text{CH}_3\text{CN}$ species, which show a single upfield hydrido resonance in the ^1H NMR spectra (Table 1). However, this solvato species could not be isolated as such in the solid state, which suggests the presence of dinuclear species also in solid $\mathbf{3}$. Some support for this hypothesis comes from a study of the IR spectra (ATR) of the complexes, which show strong vibrations around 1675–1550

Table 1. Observed Chemical Shifts for the Hydrido Ligand in the ^1H NMR Spectra of $[\text{IrH}(\kappa^3\text{-hqca})(\text{coe})(\text{L})]$ ($\mathbf{3}\cdot\text{L}$) Species at 298 K

L	deuterated solvent	δ (ppm)
THF	THF- d_8	−36.26
CH_3OH	C_6D_6	−34.24
CH_3OH	THF- d_8	−34.70
CH_3CN	THF- d_8	−29.44
CH_3CN	toluene- d_8	−28.34
py ^a	CD_2Cl_2	−26.48

^aCompound $[\text{IrH}(\kappa^3\text{-hqca})(\text{coe})(\text{py})]$ ($\mathbf{4}$).

and 1450 cm^{-1} corresponding to the asymmetric and symmetric stretching modes of the carboxylate group, respectively.²⁸ In particular, the asymmetric stretching mode of higher energy, in the $1675\text{--}1637\text{ cm}^{-1}$ range for the complexes reported herein, was observed at an unusually low frequency of 1615 cm^{-1} in the ATR spectrum of **3**.²⁹ In contrast, this absorption was observed at 1683 cm^{-1} in THF solution.

The chemical shift of a hydride ligand coordinated to a transition metal is sensitive to the donor atom in a *trans* position.³⁰ In general, a high-field shift of $\delta(\text{Ir}\text{--}\text{H})$ with a decrease in the donor strength of the *trans* ligand L has been observed in *trans*- $[\text{IrCl}(\text{CO})\text{H}(\text{PPh}_3)_2\text{L}]$ complexes.³¹ However, the data in Table 1 show a reverse tendency for $\text{L} = \text{CH}_3\text{CN}$, CH_3OH , THF, in comparison with the donor number of the solvent,³² pyridine being out of the trend as it shows a notable downfield shift (see the Supporting Information).

These observations point to a weak solvent interaction in the solvates $[\text{IrH}(\kappa^3\text{-hqca})(\text{coe})(\text{L})]$ (**3-L**; $\text{L} = \text{CH}_3\text{CN}$, CH_3OH , THF) and a strong interaction in the pyridine adduct. In fact, we were able to isolate $[\text{IrH}(\kappa^3\text{-hqca})(\text{coe})(\text{py})]$ (**4**) in the solid state (see below). In order to test this hypothesis, the standard free energy changes, ΔG° (kcal mol^{-1}), for the formation of species **3-L** from the unsaturated complex **3** were calculated. As can be observed in Table 2, the formation of **3-py**

Table 2. Calculated ΔG° (kcal mol^{-1}) for the Formation of the Species $[\text{IrH}(\kappa^3\text{-hqca})(\text{coe})(\text{L})]$ (**3-L**) from the Unsaturated Complex $[\text{IrH}(\kappa^3\text{-hqca})(\text{coe})]$ (**3**)

L	THF	CH_3CN	CH_3OH	py
ΔG° (kcal mol^{-1})	+0.61	-2.19	-3.16	-6.65

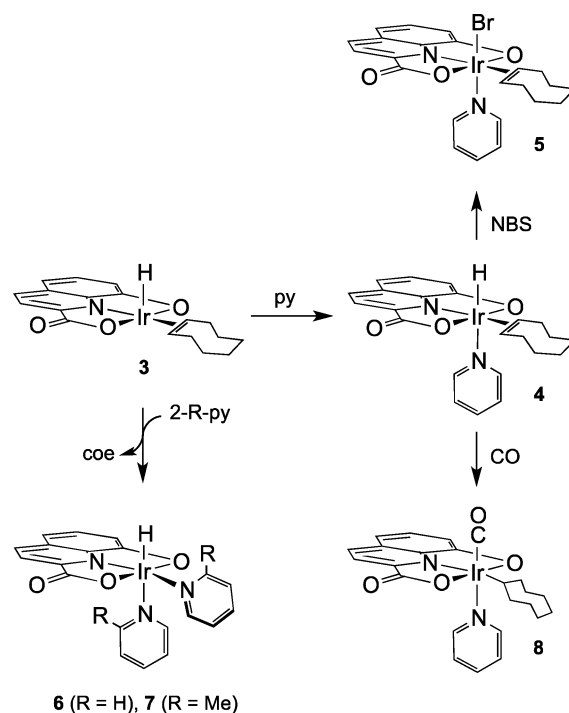
(compound **4**) is strongly thermodynamically favored but the formation of **3-THF** is slightly unfavorable. Interestingly, this latter result further supports the interpretation of DOSY experiments, in particular, the better adjustment of the calculated radius ratio to the experimentally determined value when using $r_{\text{H}}(\text{3})$ instead of $r_{\text{H}}(\text{3-THF})$ (see above).

The formation of $[\text{IrH}(\kappa^3\text{-hqca})(\text{coe})]$ (**3**) supports the hydrido/insertion route proposed for the formation of the σ,π -cyclooctenyl complex $[\text{Ir}(\kappa^3\text{-hqca})(1-\kappa-4,5-\eta\text{-C}_8\text{H}_{13})]$ (**1**). The very different outcomes in the protonation reactions of the dinuclear complexes $[\text{Ir}(\mu\text{-OMe})(\text{cod})]_2$ and $[\text{Ir}(\mu\text{-OH})(\text{cod})]_2$ with H_2hqca are a consequence of the distinct chemical behavior of the related octahedral hydrido intermediates $[\text{IrH}(\kappa^3\text{-hqca})(\text{cod})]$ and $[\text{IrH}(\kappa^3\text{-hqca})(\text{coe})_2]$ with a *mer* disposition of the 8-oxidoquinoline-2-carboxylato ligand. The high *trans* influence of the hydrido ligand promotes the cyclooctene dissociation in $[\text{IrH}(\kappa^3\text{-hqca})(\text{coe})_2]$ to give **3**. In contrast, the formation of the methanol adduct $[\text{IrH}(\kappa^2\text{-hqca})(\text{cod})(\text{CH}_3\text{OH})]$ paves the way to the hydrido migration to the cod ligand, leading to **1**.¹⁶

Reactivity of $[\text{IrH}(\eta^3\text{-hqca})(\text{coe})]$. The presence of a coordination vacant site and a replaceable coe ligand in $[\text{IrH}(\kappa^3\text{-hqca})(\text{coe})]$ (**3**) has prompted us to study its reactivity with N- and P-donor ligands. Reaction of **3** with triphenylphosphine gave an intractable mixture of several hydrido-containing products. In contrast, reaction with an excess of

pyridine at room temperature cleanly gave the octahedral adduct $[\text{IrH}(\kappa^3\text{-hqca})(\text{coe})(\text{py})]$ (**4**), which was isolated as an orange-red solid in excellent yield. The coordination of pyridine became evident in the ^1H NMR spectrum, where the expected set of resonances for the 8-oxidoquinoline-2-carboxylato and coe ligands was also observed. The stereochemistry of **4** was unequivocally established by means of the $^1\text{H}\text{--}^1\text{H}$ NOESY spectrum, which showed cross peaks between the hydrido ligand and the nearest $>\text{CH}_2$ protons of the coe ligand and between the *ortho* pyridine protons and the $=\text{CH}$ coe protons. Thus, the hydrido and pyridine ligands in **4** are disposed mutually *trans*, thereby confirming that the py ligand occupies the vacant position in **3** (Scheme 4). In fact, a high-field shift of

Scheme 4. Reactivity of $[\text{IrH}(\kappa^3\text{-hqca})(\text{coe})]_2$ (**3**)



the hydrido resonance was seen in the ^1H NMR spectrum upon coordination of the pyridine ligand, which was observed at -26.48 ppm (Table 1). In addition, the Ir–H stretching frequency in the IR spectrum was observed at 2211 cm^{-1} , shifted to lower energies in comparison to **3**.

Compound **4** was readily converted into the bromo derivative $[\text{IrBr}(\kappa^3\text{-hqca})(\text{coe})(\text{py})]$ (**5**) in dichloromethane at room temperature by using N-bromosuccinimide as hydride acceptor. Compound **5** was isolated as an orange solid in moderate yield and has been fully characterized by NMR spectroscopy and FAB mass spectroscopy. In particular, the cross peaks observed in the $^1\text{H}\text{--}^1\text{H}$ NOESY NMR spectrum evidenced the mutually *cis* disposition of both coe and pyridine ligands. Surprisingly, we have observed that **4** slowly decomposes in CH_2Cl_2 in the presence of MeOH to give the bis-pyridine complex $[\text{IrH}(\kappa^3\text{-hqca})(\text{py})_2]$ (**6**) and other unidentified byproducts. Interestingly, **6** was prepared from **3** and an excess of pyridine under more forcing conditions (THF, 70°C , 12 h). In contrast, reaction of **3** with a large excess of 2-methylpyridine in THF at room temperature directly gave $[\text{IrH}(\kappa^3\text{-hqca})(2\text{-Mepy})_2]$ (**7**), which points to a labile cyclooctene ligand in the likely intermediate $[\text{IrH}(\kappa^3\text{-hqca})\text{--}$

(coe)(2-Mepy)]. In sharp contrast, the bromo derivative **5** is inert and was recovered unaltered after refluxing for 2 h in neat pyridine.

The pyridine derivatives **6** and **7** were isolated as orange-red solids in yields of over 90% and were fully characterized by NMR spectroscopy. The ^1H NMR spectra of the complexes showed the presence of two nonequivalent pyridine ligands and the expected high-field resonance for the hydrido ligand at -23.31 (**6**) and -26.06 ppm (**7**). The different pyridine ligands, *cis* and *trans* to the hydrido ligand, have been unambiguously identified with the help of two-dimensional NMR techniques and, in particular, the NOE effect between the hydrido ligand and the *ortho* pyridine protons in the *cis* pyridine ligand. The structure of **6** has been determined by a single-crystal X-ray analysis and is shown in Figure 5. The iridium

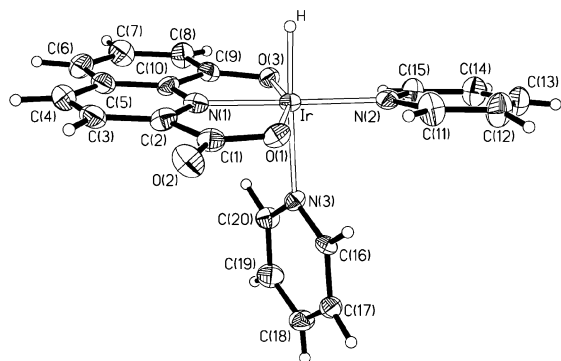


Figure 5. Molecular structure of $[\text{IrH}(\kappa^3\text{-hqca})(\text{py})_2]$ (**6**). Selected bond distances (Å) and angles ($^\circ$): Ir–O(1) = 2.098(4), Ir–O(3) = 2.086(4), Ir–N(1) = 1.954(6), Ir–N(2) = 2.045(6), Ir–N(3) = 2.172(5), Ir–H = 1.62(2), C(1)–O(1) = 1.319(8), C(1)–O(2) = 1.221(8), C(9)–O(3) = 1.355(8); O(1)–Ir–O(3) = 160.00(18), O(1)–Ir–N(1) = 78.8(2), O(1)–Ir–N(2) = 102.0(2), O(1)–Ir–N(3) = 87.93(18), O(1)–Ir–H = 90(3), O(3)–Ir–N(1) = 81.4(2), O(3)–Ir–N(2) = 97.8(2), O(3)–Ir–N(3) = 90.37(18), O(3)–Ir–H = 92(3), N(1)–Ir–N(2) = 178.9(2), N(1)–Ir–N(3) = 93.3(2), N(1)–Ir–H = 89(3), N(2)–Ir–N(3) = 87.5(2), N(2)–Ir–H = 90(3), N(3)–Ir–H = 177(3).

center exhibits a distorted-octahedral coordination, having the rigid doubly deprotonated ONO-tridentate ligand in a meridional position together with a pyridine ligand; an additional pyridine group and hydrido ligand—mutually *trans* disposed—complete the metal environment. As observed in **1a** and in the related pyridinedicarboxylate analogue $[\text{Ir}(\kappa^3\text{-pydc})(1-\kappa-4,5-\eta\text{-C}_8\text{H}_{13})(\text{MeOH})]$,¹⁵ the main distortion arises from the doubly chelating coordination of the tridentate ligand, which shows a O(1)–Ir–O(3) angle of $160.00(18)^\circ$.

The Ir–N bond distances of the three different pyridine moieties spread over a broad range (1.954–2.172 Å), reflecting their diverse electronic nature and structural disposition; while the nitrogen of the quinoline, N(1), involved in two chelating units exhibits the shortest Ir–N bond length, 1.954(6) Å, the nitrogen N(3) of the pyridine disposed *trans* to the high *trans* effect hydrido ligand³³ shows the longest value, 2.172(5) Å.

The hydrido complexes **4** and **6** undergo fast pyridine exchange with $\text{py}-d_5$ (*) at room temperature. In both cases, monitoring of CD_2Cl_2 solutions of the complexes (0.020 M) after addition of a 5-fold excess of $\text{py}-d_5$ showed an equilibria of **4/4*** and **6/6*** after approximately 15 min. Interestingly, the ^1H NMR revealed that pyridine exchange in $[\text{IrH}(\kappa^3\text{-hqca})(\text{py})_2]$ (**6**) exclusively takes place *trans* to the hydrido ligand.

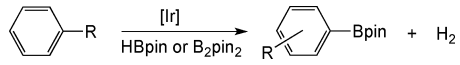
This result is a consequence of the *trans* effect exerted by the hydrido ligand and is in full agreement with the structural parameters found in the solid-state structure of **6**.

On the other hand, the hydrido ligand in $[\text{IrH}(\kappa^3\text{-hqca})(\text{coe})(\text{py})]$ (**4**) undergoes H/D exchange at a much slower rate than in $[\text{IrH}(\kappa^3\text{-hqca})(\text{coe})]$ (**3**). In fact, complete hydrido H/D exchange was observed in $\text{CD}_2\text{Cl}_2/\text{MeOH}-d_4$ (1/3) at room temperature in a few minutes in **3** and after 72 h in **4**. In sharp contrast, no H/D exchange was observed in compound **6**. These results denote the stronger acid character of the hydrido ligand in **3** in comparison to **4** and **6**.³⁴ This was further confirmed by a natural bond orbital (NBO) analysis³⁵ of the charge on the hydrido ligand in these complexes. The NBO charge in **3** was +0.12, whereas the charges in **4** and **6** were -0.03 and -0.05 , respectively.

Bubbling carbon monoxide through a solution of $[\text{IrH}(\kappa^3\text{-hqca})(\text{coe})(\text{py})]$ (**4**) at room temperature for 1.5 h gave an orange solution of the carbonyl complex $[\text{Ir}(\kappa^3\text{-hqca})(1-\kappa\text{-C}_8\text{H}_{15})(\text{CO})(\text{py})]$ (**8**) (Scheme 4). Under similar reaction conditions, carbonylation of **3** gave unsoluble unidentified products. The attempts to isolate **8** in the solid state were unsuccessful, as it decomposed to several unidentified hydrido species in the absence of a carbon monoxide atmosphere. Thus, the characterization of **8** has been carried out in solution (CD_2Cl_2) under a carbon monoxide atmosphere at 233 K. The aromatic part of the ^1H NMR spectrum showed the characteristic resonances of the tridentate ONO and pyridine ligands and a set of resonances between 1.80 and 1.10 ppm corresponding to the cyclooctenyl ligand. The carbonyl ligand in **8** was observed at 2031 cm^{-1} in the IR spectrum and at δ 173.83 ppm in the $^{13}\text{C}\{^1\text{H}\}$ NMR spectrum. The presence of a 1- κ -cyclooctenyl ligand was further confirmed in the ^{13}C ATP NMR spectrum, which showed the Ir–CH resonance at 21.61 ppm and a set of seven resonances for the $>\text{CH}_2$ protons. Most probably, the formation of **8** involves (i) the replacement of the pyridine ligand in **4** by carbon monoxide to give $[\text{IrH}(\kappa^3\text{-hqca})(\text{coe})(\text{CO})]$, (ii) migratory insertion of the coe ligand into the Ir–H bond, and (iii) fast coordination of pyridine at the resulting vacant site.

Catalytic Borylation of Arenes. The iridium-catalyzed borylation of arene C–H bonds is one of the most practically useful methods for C–H functionalization.¹² Recently, some pincer iridium(III) and salicylaldimine iridium(I) complexes with catalytic activity in C–H borylation of arenes have been reported.^{36,37} Interestingly, the 8-oxidoquinoline-2-carboxylate iridium(III) pincer complexes efficiently catalyzed the arene C–H borylation under thermal conditions.

The catalytic activity of complexes **1**–**5** in the borylation of arenes using HBpin as borylating reagent was evaluated (Table 3). The reactions were carried out in neat arene using a catalyst loading of 5.0 mol % in the 60–90 °C temperature range. The σ,π -cyclooctenyl unsaturated complex $[\text{Ir}(\kappa^3\text{-hqca})(1-\kappa-4,5-\eta\text{-C}_8\text{H}_{13})]$ (**1**) showed a low activity in the borylation of benzene, giving a 20% conversion in 20 h at 90 °C (entry 1). However, an activity increase, 64%, was observed with the pyridine precursor $[\text{Ir}(\kappa^3\text{-hqca})(1-\kappa-4,5-\eta\text{-C}_8\text{H}_{13})(\text{py})]$ (**2**) under the same conditions (entry 2). The positive influence of the presence of a pyridine ligand in the catalyst precursor was also observed with the cyclooctene complexes $[\text{IrH}(\kappa^3\text{-hqca})(\text{coe})]$ (**3**) and $[\text{IrH}(\kappa^3\text{-hqca})(\text{coe})(\text{py})]$ (**4**). The precursor **3** gave 38% of PhBpin, whereas a conversion of 72% was attained with **4** (entries 3 and 6). It is remarkable that no catalytic activity was observed below 60 °C, with a steady increase in conversion

Table 3. Aromatic C–H Borylation Catalyzed by Iridium 8-Oxidoquinoline-2-carboxylate Pincer Complexes^a


entry	catalyst	arene	boron reagent	T (°C)	yield (%) ^b (o:m:p)
1	1	R = H	HBpin	90	20
2	2		HBpin	90	64
3	3		HBpin	90	38
4	4		HBpin	60	37
5	4		HBpin	70	63
6	4		HBpin	90	72
7	4		B ₂ pin ₂	90	70
8	5		HBpin	90	9
9	4	R = CF ₃	HBpin	90	88 (0.70:30)
10	4	R = OMe	HBpin	90	71 (6.69:25)
11	7	R = OMe	HBpin	90	59 (8.66:26)

^aReaction conditions: arene (22 mmol), HBpin (0.146 mmol) or B₂pin₂ (0.073 mmol), catalyst (0.0037 mmol) without solvent for 20 h.

^bYields, based on boron atom, and isomer ratios were determined by ¹H NMR.

with increasing temperature (entries 4 and 6). Interestingly, similar conversion was achieved when using B₂pin₂ as borylating reagent (2.5 mol % of catalyst in order to maintain the B/Ir ratio), indicating that both boryl groups participate in the reaction (entry 7). The bromo complex [IrBr(κ³-hqca)-(coe)(py)] (5) showed very little catalytic activity (entry 8).

The 8-oxidoquinoline-2-carboxylato iridium(III) pincer complexes exhibited a slightly better performance than those of the related 2,6-pyridinedicarboxylate (pydc). Although 3 and [IrH(κ³-pydc)(coe)] (39%) showed comparable activities (entry 3), 4 is more active than [IrH(κ³-pydc)(coe)(py)] (63%) under the same conditions (entry 6).¹⁵ In contrast to the case for 4 (entry 7), [IrH(κ³-pydc)(coe)(py)] showed no catalytic activity at 90 °C when using B₂pin₂ as borylating reagent, although good conversion to PhBpin was attained at much higher temperatures: 4% at 100 °C and 82% at 110 °C.

Reactions of monosubstituted arenes Ph–R (R = OMe, CF₃) with HBpin under the standard catalytic conditions afforded a mixture of borylated products. The borylation of trifluoromethylbenzene with 4 as catalyst precursor gave the *meta*- and *para*-disubstituted products in 88% with a *meta:para* ratio of 2.3 (entry 9). This isomer ratio is slightly over the statistical ratio of 2.0 and is lower than that observed with other iridium catalysts, such as the Ir/bipyridine system.³⁸ The lack of an *ortho* isomer could be ascribed to the steric effect introduced by the bulky substituent. The borylation of anisole provided an isomer mixture with 6% of the *ortho* product, probably due to the directing effect of the methoxy group, and a *meta:para* ratio of 2.8 (entry 10). In general, the bis-pyridine complex [IrH(κ³-hqca)(2-Mepy)₂] (7) is less active than 4. Thus, the borylation of anisole catalyzed by 7 (entry 11) gave a 59% conversion with similar regioselectivity.

Although we have no clear evidence for the catalytic reaction mechanism, a common boryl intermediate, [Ir(κ³-hqca)(Bpin)-L], generated by reactions of the different catalyst precursors with HBpin or B₂pin₂, might be involved in C–H bond activation. [IrH(κ³-hqca)(coe)] (3) has a remarkable thermal stability, as it can be recovered unaltered after heating in C₆D₆ for 14 h at 120 °C with no observable H/D exchange. However, 3 reacts with HBpin in tetrahydrofuran or dichloromethane but, unfortunately, we were not able to identify or

isolate any well-defined boryl derivatives. On the other hand, neither [Ir(μ-OH)(coe)₂] nor [Ir(κ²-hq)(coe)₂] (hq = 8-hydroxyquinolinato) showed significant catalytic activity in the borylation of benzene with B₂pin₂ at 90 °C, which points to the involvement of the tridentate ligand in the catalytically active species. In fact, the formation of [Ir(κ³-hqca)(Bpin)(coe)] could take place by reaction of HBpin with the unsaturated σ,π-cyclooctenyl complex 1 or with the hydrido complex 3 after molecular hydrogen release. The resulting 16-electron square-pyramidal species with a boryl ligand in the apical position, due to its very strong *trans* influence,³⁹ could be further stabilized by coordination of pyridine and release of cyclooctene, accounting for the positive effect of the pyridine ligand on the catalytic activity. This unsaturated species could be competent for C–H borylation reactions through a mechanism similar to that operative in the Ir/dtbp catalytic system (dtbp = 4,4'-di-*tert*-butyl-2,2'-bipyridine) involving the trisboryl iridium(III) species [Ir(dtbp)(Bpin)₃].⁴⁰

CONCLUSIONS

8-Hydroxyquinoline-2-carboxylic acid allows for the synthesis of unsaturated iridium(III) pincer complexes containing the 8-oxidoquinoline-2-carboxylato ligand. The 16-electron complexes [Ir(κ³-hqca)(1-κ-4,5-η-C₈H₁₃)] and [IrH(κ³-hqca)(coe)] have been prepared from standard mono- and dinuclear iridium complexes. The key to the formation of the two very different complexes is the chemical behavior of the hydrido intermediates [IrH(κ³-hqca)(cod)] and [IrH(κ³-hqca)(coe)₂]. Hydrido migration to the cod ligand in the former and cyclooctene dissociation in the latter result in the formation of the unsaturated σ,π-cyclooctenyl and hydrido complexes, respectively. [IrH(κ³-hqca)(coe)] exists as dinuclear assemblies of square-pyramidal iridium(III) hydrido complexes both in the solid state and in nonpolar solvents but as the corresponding solvates in polar solvent solutions. In contrast, the dimerization of the σ,π-cyclooctenyl complex was not observed, probably due to the steric interference of the bulky cyclooctenyl ligands. These complexes efficiently catalyzed arene C–H borylation under thermal conditions, the octahedral pyridine adducts being more active than the corresponding unsaturated complexes. Most probably, the catalytic reaction mechanism involves the participation of a unsaturated monoboryl iridium(III) species.

EXPERIMENTAL SECTION

Synthesis. All experiments were carried out under an atmosphere of argon using Schlenk techniques or a glovebox. Liquid or solution transfers between reaction vessels were done via cannula. Solvents were obtained from a Solvent Purification System (Innovative Technologies). CD₂Cl₂, benzene-*d*₆, and toluene-*d*₈ (Euriso-top) were dried using activated molecular sieves. Methanol-*d*₄ (<0.02% D₂O, Euriso-top) was used as received. Standard literature procedures were used to prepare the starting materials [Ir(μ-OMe)(cod)]₂⁴¹ and [Ir(μ-OH)(coe)₂]₂.⁴² 8-Hydroxyquinoline-2-carboxylic acid (H₂hqca) was obtained from Aldrich and used as received. Pinacolborane (HBpin) and bis(pinacolato)diboron (B₂pin₂) were obtained from Aldrich and used as received.

Scientific Equipment. Elemental analyses were carried out with a PerkinElmer 2400 CHNS/O analyzer. NMR spectra were recorded on Bruker AV-400 and AV-300 spectrometers. Chemical shifts are reported in ppm relative to tetramethylsilane and referenced to partially deuterated solvent resonances. Coupling constants (*J*) are given in hertz. Spectral assignments were achieved by combination of ¹H–¹H COSY, NOESY, ¹³C DEPT and APT, ¹H–¹³C HSQC, and

^1H – ^{13}C HMBC experiments. Electrospray mass spectra (ESI-MS) were recorded on a Bruker MicroTof-Q instrument using sodium formate as reference. MALDI-TOF mass spectra were obtained on a Bruker Microflex mass spectrometer using DCTB (*trans*-2-[3-(4-*tert*-butylphenyl)-2-methyl-2-propenyldiene]malononitrile) or dithranol as the matrix. FT-IR spectra were collected on a Nicolet Nexus 5700 FT spectrophotometer equipped with a Nicolet Smart Collector diffuse reflectance accessory. The numbering scheme for NMR data is given in Figure 6.

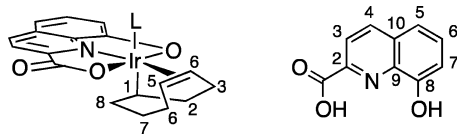


Figure 6. Numbering scheme for NMR data.

Synthesis of $\text{Li}_2[\text{hqca}]$. *n*-BuLi (5.0 mL, 8 mmol, 1.6 M) was added dropwise to a suspension of 8-hydroxyquinoline-2-carboxylic acid (0.757 g, 4.00 mmol) in diethyl ether (50 mL) with stirring at 195 K. The reaction mixture was warmed to room temperature for 1 h. The resulting suspension was concentrated under vacuum, and then diethyl ether (15 mL) was added, leading to the precipitation of a yellow solid, which was filtered, washed with diethyl ether, and dried in vacuo. Yield: 0.771 g (96%). ^1H NMR (400.16 MHz, 298 K, $\text{CD}_2\text{Cl}_2/\text{CD}_3\text{OD}$): δ 8.25 (d, 1H, $J_{\text{H-H}} = 8.8$ Hz, H-4), 8.08 (d, 1H, $J_{\text{H-H}} = 8.8$ Hz, H-3), 7.46 (t, 1H, $J_{\text{H-H}} = 8.1$ Hz, H-6), 7.32 (d, 1H, $J_{\text{H-H}} = 8.1$ Hz, H-5), 7.09 (d, 1H, $J_{\text{H-H}} = 8.1$ Hz, H-7). Anal. Calcd for $\text{C}_{10}\text{H}_5\text{Li}_2\text{NO}_3$: C, 59.74; H, 2.51; N, 6.97. Found: C, 59.68; H, 2.62; N, 6.95.

Synthesis of the Complexes. $[\text{Ir}(\kappa^3\text{-hqca})(1-\kappa\text{-}4,5\text{-}\eta\text{-}\text{C}_8\text{H}_{13})]$ (**1a**). A mixture of $[\text{Ir}(\mu\text{-OMe})(\text{cod})]_2$ (0.166 g, 0.250 mmol) and 8-hydroxyquinoline-2-carboxylic acid (0.095 g, 0.502 mmol) was dissolved in $\text{CH}_2\text{Cl}_2/\text{MeOH}$ (3/1, 40 mL). The yellow solution was stirred overnight at room temperature to give a dark red solution. The solution was filtered and then concentrated in vacuo to ca. 5 mL. Slow addition of diethyl ether gave the compound as a red solid, which was filtered, washed with diethyl ether, and dried in vacuo. The crude compound was dissolved in a $\text{CH}_2\text{Cl}_2/\text{MeOH}$ (3/1) mixture and then eluted through an alumina column (14×1.5 cm) to give a red solution. Concentration of the solution and addition of diethyl ether afforded a red microcrystalline solid that was filtered, washed with diethyl ether, and dried in vacuo. Yield: 88% (0.230 g, 1-MeOH). Anal. Calcd for $\text{C}_{18}\text{H}_{18}\text{IrNO}_3 \cdot \text{MeOH}$: C, 43.83; H, 4.26; N, 2.69. Found: C, 43.75; H, 4.31; N, 2.64. MS (MALDI, CH_2Cl_2 , m/z): 487.9 $[\text{M}]^+$. ^1H NMR (400.162 MHz, 298 K, $\text{CD}_3\text{OD}/\text{CD}_2\text{Cl}_2$): δ 8.21 (d, 1H, $J_{\text{H-H}} = 8.7$ Hz, H-4), 7.74 (d, 1H, $J_{\text{H-H}} = 8.7$ Hz, H-3), 7.42 (t, 1H, $J_{\text{H-H}} = 8.1$ Hz, H-6), 7.0 (d, 1H, $J_{\text{H-H}} = 8.1$ Hz, H-5), 6.82 (d, 1H, $J_{\text{H-H}} = 8.1$ Hz, H-7) (hqca), 5.73 (td, $J_{\text{H-H}} = 9.2$, 4.0 Hz, 1H, H-4), 5.54 (dd, $J_{\text{H-H}} = 9.1$, 3.0 Hz, 1H, H-5), 3.07 (d, $J_{\text{H-H}} = 18.2$ Hz, 1H, H-6), 2.36 (m, 1H, H-3), 2.23–2.11 (m, 2H, H-3 and H-6), 2.06 (m, 1H, H_2), 1.84 (ddt, $J_{\text{H-H}} = 23.3$, 13.3, 4.6 Hz, 1H, H-7), 1.59 (d, $J_{\text{H-H}} = 13.2$ Hz, 1H, H-7), 1.04 (t, $J_{\text{H-H}} = 8.1$ Hz, 1H, H-8), 0.78 (m, $J_{\text{H-H}} = 8.02$, H-1), 0.28 (dd, $J_{\text{H-H}} = 12.9$, 8.8 Hz, 1H, H-2), –0.02 (m, 1H, H-8) (C_8H_{13}). $^{13}\text{C}\{^1\text{H}\}$ NMR (75.48 MHz, 298 K, $\text{CD}_3\text{OD}/\text{CD}_2\text{Cl}_2$): δ 176.65 (C=O), 171.05 (C-8), 144.53 (C-2), 141.57 (C-9), 137.05 (C-6), 133.97 (C-4), 133.22 (C-10), 122.09 (C-3), 115.60 (C-7), 113.89 (C-5) (hqca), 87.80 (C-4), 82.98 (C-5), 40.03 (C-2), 34.64 (C-8), 27.42 (C-6), 25.93 (C-3), 24.54 (C-7), 13.19 (C-1) (C_8H_{13}). IR (ATR, cm^{-1}): $\nu(\text{CO})$ 1637 (s).

$[\text{Ir}(\kappa^3\text{-hqca})(1-\kappa\text{-}4,5\text{-}\eta\text{-}\text{C}_8\text{H}_{13})]$ (**1a,b**). A solid mixture of $[\text{Ir}(\text{cod})-(\text{CH}_3\text{CN})_2]\text{BF}_4$ (0.235 g, 0.500 mmol) and $[\text{Li}_2\text{hqca}]$ (0.100 g, 0.500 mmol) was dissolved in $\text{CH}_2\text{Cl}_2/\text{MeOH}$ (3/1, 40 mL). The solution was stirred overnight at room temperature, resulting in a color change from red to dark red. The solution was filtered through Celite and then concentrated in vacuo to ca. 5 mL. Addition of diethyl ether afforded the compound as a red solid, which was washed with diethyl ether and dried in vacuo. Yield: 92% (0.240 g of 1-MeOH). NMR spectroscopic

data evidenced the formation of **1** as an isomer mixture, **1a,b**, in a 1:1 ratio. When the reaction was carried out in $\text{CH}_2\text{Cl}_2/\text{MeOH}/\text{H}_2\text{O}$ (30/10/0.5, 40.5 mL), an isomer mixture containing 70% of **1a** was obtained. NMR data for isomer **1b** are as follows. ^1H NMR (400.162 MHz, 298 K, $\text{CD}_3\text{OD}/\text{CD}_2\text{Cl}_2$): δ 8.21 (d, 1H, $J_{\text{H-H}} = 8.6$ Hz, H-4), 7.77 (d, 1H, $J_{\text{H-H}} = 8.6$ Hz, H-3), 7.43 (t, 1H, $J_{\text{H-H}} = 8.1$ Hz, H-6), 6.97 (d, 1H, $J_{\text{H-H}} = 8.1$ Hz, H-5), 6.84 (d, 1H, $J_{\text{H-H}} = 8.1$ Hz, H-7) (hqca), 5.74 (td, 1H, $J = 8.8$, 3.6 Hz, =CH), 5.51 (dd, 1H, $J_{\text{H-H}} = 13.4$, 3.3 Hz, =CH), 3.11 (d, 1H, $J_{\text{H-H}} = 13.1$ Hz, >CH₂), 2.44–0.94 (set of m, 8H, >CH₂), 0.35 (dd, 1H, $J_{\text{H-H}} = 12.6$, 8.6 Hz), –0.13 (m, 1H, $J_{\text{H-H}} = 13.9$, 4.0 Hz) (C_8H_{13}). $^{13}\text{C}\{^1\text{H}\}$ NMR (75.48 MHz, 298 K, $\text{CD}_3\text{OD}/\text{CD}_2\text{Cl}_2$): δ 176.06 (C=O), 170.01 (C-8), 136.02 (C-6), 133.30 (C-4), 132.29 (C-10), 121.44 (C-3), 114.97 (C-7), 113.03 (C-5) (hqca), 80.31 (C-4), 82.17 (C-5), 39.05, 33.44, 26.17, 25.19, 23.71 (>CH₂), 13.16 (CH–Ir) (C_8H_{13}).

$[\text{Ir}(\kappa^3\text{-hqca})(1-\kappa\text{-}4,5\text{-}\eta\text{-}\text{C}_8\text{H}_{12}\text{D})]$ (**1-d₁**). A solid mixture of $[\text{Ir}(\text{cod})-(\text{CH}_3\text{CN})_2]\text{PF}_6$ (0.053 g, 0.100 mmol) and $[\text{Li}_2\text{hqca}]$ (0.021 g, 0.104 mmol) was dissolved in $\text{CD}_2\text{Cl}_2/\text{MeOH}-d_4/\text{D}_2\text{O}$ (4/2/0.1, 6.1 mL). The solution was stirred overnight at room temperature and then directly analyzed by NMR. **1a-d₁**/**1b-d₁** ratio: 65/35. $^{13}\text{C}\{^1\text{H}\}$ NMR (75.47 MHz, 298 K, $\text{CD}_3\text{OD}/\text{CD}_2\text{Cl}_2$): selected resonances, δ 33.64 (t, $J_{\text{D-C}} = 20.6$ Hz, C-8, **1a-d₁**), 33.50 (t, $J_{\text{D-C}} = 20.6$ Hz, C-8, **1b-d₁**).

$[\text{Ir}(\kappa^3\text{-hqca})(1-\kappa\text{-}4,5\text{-}\eta\text{-}\text{C}_8\text{H}_{13})(\text{py})]$ (**2a**). $[\text{Ir}(\kappa^3\text{-hqca})(1-\kappa\text{-}4,5\text{-}\eta\text{-}\text{C}_8\text{H}_{13})]$ (**1a**-MeOH; 0.104 g, 0.200 mmol) was dissolved in neat pyridine (4 mL) and gently refluxed for 4 h. The solvent was removed under vacuum, the residue was dissolved in dichloromethane (5 mL), and the solution was filtered through a silica gel pad. The red solution was concentrated, and diethyl ether (20 mL) was added to give a red solid, which was filtered, washed with diethyl ether (3×10 mL), and dried in vacuo. Yield: 91% (0.103 g). Anal. Calcd for $\text{C}_{23}\text{H}_{23}\text{IrN}_2\text{O}_3$: C, 48.66; H, 4.08; N, 4.93. Found: C, 48.74; H, 4.03; N, 4.57. MS (MALDI, CH_2Cl_2 , m/z): 487.9 $[\text{M} - \text{py}]^+$. ^1H NMR (400.162 MHz, 298 K, CD_2Cl_2): δ 8.48 (dt, 2H, $J_{\text{H-H}} = 4.8$, 1.5 Hz, *o*-H, py), 7.98 (d, 1H, $J_{\text{H-H}} = 8.6$ Hz, H-4), 7.60 (d, 1H, $J_{\text{H-H}} = 8.6$ Hz, H-3) (hqca), 7.59 (tt, 1H, $J = 7.8$, 1.5 Hz, *p*-H, py), 7.36 (t, 1H, $J_{\text{H-H}} = 8.1$ Hz, H-6, hqca), 7.22 (m, 2H, $J_{\text{H-H}} = 6.6$, 1.5 Hz, *m*-H, py), 6.85 (d, 2H, $J_{\text{H-H}} = 8.1$ Hz, H-5), 6.75 (d, 2H, $J_{\text{H-H}} = 8.1$ Hz, H-7) (hqca), 5.43 (td, 1H, $J_{\text{H-H}} = 8.8$, 3.6 Hz, =CH), 5.00 (bd, 1H, $J_{\text{H-H}} = 9.1$ Hz, =CH), 2.98 (d, 1H, $J_{\text{H-H}} = 16.2$ Hz), 2.5–2.1 (set of m), 1.99 (t, 1H, $J_{\text{H-H}} = 3.0$ Hz), 1.90–1.75 (m, 1H), 1.62 (br, 1H), 1.34–1.16 (bm, 1H), 0.63 (dd, 1H, $J_{\text{H-H}} = 11.4$, 8.7 Hz), 0.39 (m, 1H) (C_8H_{13}). $^{13}\text{C}\{^1\text{H}\}$ NMR (100.62 MHz, 298 K, CD_2Cl_2): δ 174.71 (C=O), 171.45 (C-8) (hqca), 149.03 (2C, py), 143.36 (C-2), 140.69 (C-9) (hqca), 137.97 (py), 135.73 (C-6), 133.33 (C-4), 132.72 (C-10) (hqca), 125.96 (2C, py), 121.90 (C-3), 115.15 (C-7), 113.03 (C-5) (hqca), 87.57, 82.70 (=CH), 39.27, 33.94, 27.16, 27.06, 24.18 (>CH₂), 14.62 (CH–Ir) (C_8H_{13}). IR (ATR, cm^{-1}): $\nu(\text{CO})$ 1660 (s).

$[\text{Ir}(\kappa^3\text{-hqca})(1-\kappa\text{-}4,5\text{-}\eta\text{-}\text{C}_8\text{H}_{13})(\text{py})]$ (**2a,b**). An isomer mixture of $[\text{Ir}(\kappa^3\text{-hqca})(1-\kappa\text{-}4,5\text{-}\eta\text{-}\text{C}_8\text{H}_{13})]$ (0.104 g, 0.200 mmol, **1a/1b** = 70/30) was dissolved in neat pyridine (4 mL) and gently refluxed for 4 h. Workup as described above gave the compound as an isomer mixture (**2a/2b** = 74/26). Yield: 87% (0.099 g). NMR data for isomer **2b** are as follows. ^1H NMR (400.162 MHz, 298 K, CD_2Cl_2): δ 8.47 (dt, 2H, $J_{\text{H-H}} = 4.8$ 1.5 Hz, *o*-H, py), 7.98 (d, 1H, $J_{\text{H-H}} = 8.6$ Hz, H-4), 7.60 (d, 1H, $J_{\text{H-H}} = 8.6$ Hz, H-3) (hqca), 7.59 (tt, 1H, $J_{\text{H-H}} = 7.8$, 1.5 Hz, *p*-H, py), 7.37 (t, 1H, $J_{\text{H-H}} = 8.1$ Hz, H-6, hqca), 7.22 (m, 2H, $J_{\text{H-H}} = 6.6$, 1.5 Hz, *m*-H, py), 6.87 (d, 1H, $J_{\text{H-H}} = 7.8$ Hz, H-5), 6.84 (d, 1H, $J_{\text{H-H}} = 7.8$ Hz, H-7) (hqca), 5.47 (td, 1H, $J_{\text{H-H}} = 8.8$, 3.6 Hz, =CH), 4.95 (bd, 1H, $J_{\text{H-H}} = 8.1$ Hz, =CH), 2.98 (d, 1H, $J_{\text{H-H}} = 16.2$ Hz), 2.50–2.10 (m, 4H), 1.99 (t, 1H, $J_{\text{H-H}} = 3.0$ Hz), 1.90–1.75 (m, 1H), 1.62 (m, 1H), 1.16–1.34 (m, 1H), 0.70 (dd, $J_{\text{H-H}} = 12.9$, 8.7 Hz), 0.28 (m, 1H, $J_{\text{H-H}} = 3.5$ Hz) (C_8H_{13}). $^{13}\text{C}\{^1\text{H}\}$ NMR (100.62 MHz, 298 K, CD_2Cl_2): δ 174.63 (C=O), 170.13 (C-8) (hqca), 149.06 (2C, py), 137.97 (py), 135.65 (C-6), 133.45 (C-4), 132.58 (C-10) (hqca), 125.96 (2C, py), 122.13 (C-3), 115.34 (C-7), 112.83 (C-5) (hqca), 86.78, 83.12 (=CH), 39.27, 33.74, 27.15, 27.06, 24.28 (>CH₂), 15.73 (CH–Ir) (C_8H_{13}).

$[\text{IrH}(\kappa^3\text{-hqca})(\text{coe})]_n$ (**3**). THF (80 mL) was added to a solid mixture of $[\text{Ir}(\mu\text{-OH})(\text{coe})_2]_2$ (0.430 g, 0.500 mmol) and 8-hydroxyquinoline-2-carboxylic acid (0.189 g, 1.00 mmol). The red

solution was stirred overnight at room temperature to give a dark red solution. The solvent was removed under vacuum to give the compound as a red solid. Yield: 98% (0.480 g). Anal. Calcd for $C_{18}H_{20}IrNO_3$: C, 44.07; H, 4.11; N, 2.86. Found: C, 44.19; H, 4.34; N, 2.82. 1H NMR (400.162 MHz, 298 K, THF- d_6): δ 8.18 (d, 1H, J_{H-H} = 8.8 Hz, H-4), 7.65 (d, 1H, J_{H-H} = 8.0 Hz, H-3), 7.31 (t, 1H, J_{H-H} = 8.0 Hz, H-6), 6.84 (d, 1H, J_{H-H} = 8.0 Hz, H-5), 6.71 (d, 1H, J_{H-H} = 8.0 Hz, H-7) (hqca), 5.11 (br, 2H, =CH, coe), 2.20 (m, 2H), 2.02 (m, 2H), 1.74 (m, 4H), 1.46–1.40 (m, 4H) ($>CH_2$, coe), –36.26 (s, 1H, Ir–H) (n = 1). $^{13}C\{^1H\}$ NMR (75.468 MHz, 298 K, THF- d_6): δ 142.21 (C-9), 134.69 (C-6), 130.94 (C-4), 130.04 (C-10), 118.92 (C-3), 112.48 (C-7), 110.46 (C-5) (hqca), 80.91, 80.69 (=CH, coe), 29.66, 29.54, 26.42, 26.36, 24.70, 24.67 ($>CH_2$, coe) (n = 1). MS (MALDI, THF, m/z): 489.1 $[M - H]^+$. IR (THF, cm^{-1}): ν (Ir–H) 2269 (s); ν (CO) 1683 (s). 1H NMR (400.162 MHz, 298 K, C_6D_6): δ 7.17 (d, J_{H-H} = 8.8 Hz), 7.09 (d, J_{H-H} = 8.4 Hz), 7.01 (d, J_{H-H} = 8.8 Hz), 6.89 (t, J_{H-H} = 7.3 Hz) (hqca), 6.84–6.75 (m, hqca and 1H = CH, coe), 6.75–6.68 (m), 6.63 (d, J_{H-H} = 7.3 Hz), 6.57 (d, J_{H-H} = 8.8 Hz), 6.38 (d, J_{H-H} = 8.8 Hz) (hqca), 6.31 (br, 1H, =CH, coe), 6.28 (d, J_{H-H} = 8.4 Hz), 6.18 (t, J_{H-H} = 8.4 Hz), 6.12 (d, J_{H-H} = 7.3 Hz), 6.04 (dd, J_{H-H} = 7.0, 2.2 Hz) (hqca), 5.74 (m, 1H, J_{H-H} = 4.0 Hz), 5.66 (m, 3H, J_{H-H} = 4.4 Hz), 5.45 (m, 1H, J_{H-H} = 4.0 Hz), 4.21 (br, 1H) (=CH, coe), 2.60–0.50 (set of m, $>CH_2$, coe), –33.54 (s), –34.03 (s), –34.38 (s) –35.98 (s) (Ir–H) (n = 2). MS (ESI, toluene, m/z): 1003.2 ($M + Na^+$), 981.2 ($M + H^+$). IR (ATR, cm^{-1}): ν (Ir–H) 2255 (s); ν (CO) 1615 (s).

[Ir(κ^3 -hqca)(coe)] (3-d₁). MeOH- d_4 (15 μ L) was added to a NMR tube containing a solution of [Ir(κ^3 -hqca)(coe)] (3; 10 mg) in THF (0.6 mL). 2D NMR (61.422 MHz, 298 K, THF): δ –34.72 (s, Ir–D).

[Ir(κ^3 -hqca)(coe)(CH₃CN)] (3-CH₃CN). Acetonitrile (6 μ L) was added to a solution of [Ir(κ^3 -hqca)(coe)] (3) in toluene- d_8 (0.5 mL). 1H NMR (300.125 MHz, 223 K, toluene- d_8): δ 7.81 (bs, 1H), 7.33–7.08 (m, 3H), 6.68 (bs, 1H) (hqca), 5.68 (bs, 2H, =CH), 2.47 (bs, 2H, $>CH_2$) (coe), 2.25 (s, 3H, CH₃CN), 2.02–1.20 (m, 8H, $>CH_2$, coe), –28.34 (bs, 1H, Ir–H).

[Ir(κ^3 -hqca)(coe)(CH₃OH)] (3-CH₃OH). Compound [Ir(κ^3 -hqca)(coe)] (3; 10 mg) was dissolved in a 1/1 THF/MeOH mixture (1 mL). The solvent was removed under vacuum and the residue dissolved in C_6D_6 . 1H NMR (400.162 MHz, C_6D_6 , room temperature): δ 7.70 (d, 1H, J_{H-H} = 8.8 Hz, H-4), 7.63 (d, 1H, J_{H-H} = 8.8 Hz, H-3), 7.29 (t, 1H, J_{H-H} = 8.0 Hz, H-6), 7.07 (d, 1H, J_{H-H} = 8.0 Hz, H-5), 6.72 (d, 1H, J_{H-H} = 8.0 Hz, H-7) (hqca), 5.55 (d, 2H, J_{H-H} = 8.8 Hz, =CH-, coe), 4.60 (CH₃OH), 3.30 (t, 3H, CH₃OH), 2.60–1.50 (10H, $>CH_2$, coe), –34.24 (Ir–H).

[Ir(κ^3 -hqca)(coe)(py)] (4). Pyridine (2 mL) was added to a solution of [Ir(κ^3 -hqca)(coe)] (3; 0.245 g, 0.500 mmol) in THF (50 mL). Stirring at room temperature for 14 h afforded an orange solution. After removal of solvent, the resulting orange solid was dissolved in the minimum volume of dichloromethane (10 mL). Addition of pentane (30 mL) led to the precipitation of a red-orange solid, which was filtered, washed with pentane (3 \times 10 mL), and dried under vacuum. Yield: 97% (0.276 g). Anal. Calcd for $C_{23}H_{25}IrN_3O_3$: C, 48.49; H, 4.42; N, 4.92. Found: C, 48.33; H, 4.38; N, 4.79. MS (MALDI, CH₂Cl₂, m/z): 491.2 ($M^+ - py$). MS (ESI, CH₃CN, m/z): 569.2 $[M - H]^+$, 490.1 $[M - py - H]^+$. 1H NMR (400.162 MHz, 298 K, CD₂Cl₂): δ 8.44 (dm, 2H, J_{H-H} = 6.6 Hz, *o*-H, py), 7.97 (d, 1H, J_{H-H} = 8.0 Hz, H-4, hqca), 7.63 (tt, 1H, J_{H-H} = 6.6, 1.5 Hz, *p*-H, py), 7.58 (d, 1H, J_{H-H} = 8.0 Hz, H-3), 7.36 (t, 1H, J_{H-H} = 8.0 Hz, H-6) (hqca), 7.25 (t, 2H, J_{H-H} = 5.8 Hz, *m*-H, py), 6.88 (d, 1H, J_{H-H} = 8.0 Hz, H-5), 6.84 (d, 1H, J_{H-H} = 8.0 Hz, H-7) (hqca), 4.96 (m, 2H, =CH, coe), 2.25–2.09 (m, 4H), 1.85–1.78 (m, 2H), 1.64–1.55 (m, 2H), 1.45–1.36 (m, 4H) ($>CH_2$, coe), –26.48 (1H, Ir–H). $^{13}C\{^1H\}$ NMR (75.468 MHz, 298 K, CD₂Cl₂): δ 172.08 (C-8, hqca), 148.37, 148.19 (py), 143.57 (C-2), 142.67 (C-9) (hqca), 138.37 (py), 136.21 (C-6), 133.29 (C-4), 132.29 (C-10), (hqca), 125.97 (2C, py), 121.57 (C-3), 115.13 (C-7), 113.00 (C-5) (hqca), 83.78, 83.62 (=CH, coe), 32.31, 32.18, 29.70, 29.60, 27.12, 27.08 ($>CH_2$, coe). IR (ATR, cm^{-1}): ν (Ir–H) 2211 (s); ν (CO) 1671 (s).

[IrBr(κ^3 -hqca)(coe)(py)] (5). A mixture of [Ir(κ^3 -hqca)(coe)(py)] (4; 0.120 g, 0.211 mmol) and *N*-bromosuccinimide (0.075 g, 0.422

mmol) was dissolved in CH₂Cl₂ (20 mL) to give an orange solution, which was stirred at room temperature for 48 h. The solution was concentrated under reduced pressure to ca. 3 mL and then chromatographed on a silica gel column using CH₂Cl₂ as eluent. Concentration of the obtained solution under vacuum and addition of pentane gave the compound as an orange solid, which was filtered, washed with pentane, and dried under vacuum. Yield: 62% (0.085 g). Anal. Calcd for $C_{23}H_{24}BrIrN_2O_3$: C, 42.59; H, 3.73; N, 4.32. Found: C, 42.61; H, 3.56; N, 4.27. MS (MALDI, CH₂Cl₂, m/z): 649.1 $[M + H]^+$, 539.0 $[M - coe]^+$, 491.1 $[M - Br - py]^+$, 459.1 $[M - coe - py]^+$. 1H NMR (400.162 MHz, 298 K, CD₂Cl₂): δ 8.46 (dd, 2H, J_{H-H} = 8.8, 1.4 Hz, *o*-H, py), 8.04 (d, 1H, J_{H-H} = 8.8 Hz, H-4), 7.72 (d, 1H, J_{H-H} = 8.8 Hz, H-3) (hqca), 7.66 (m, 1H, J_{H-H} = 7.3 Hz, *p*-H, py), 7.47 (t, 1H, J_{H-H} = 8.0 Hz, H-6, hqca), 7.26 (t, 2H, J_{H-H} = 7.3 Hz, *m*-H, py), 7.05 (d, 1H, J_{H-H} = 8.0 Hz, H-5), 6.96 (d, 1H, J_{H-H} = 8.0 Hz, H-7) (hqca), 6.06 (m, 2H, =CH, coe), 2.04 (m, 2H), 1.84 (m, 2H), 1.64–1.50 (set of m, 6H), 1.28 (m, 2H) ($>CH_2$, coe). $^{13}C\{^1H\}$ NMR (75.468 MHz, 298 K, CD₂Cl₂): δ 148.77 (2C, py), 143.81 (C-9, hqca), 139.30 (py), 137.52 (C-6), 133.36 (C-4), 131.82 (C-10) (hqca), 125.69 (2C, py), 121.52 (C-3), 116.15 (C-7), 114.00 (C-5) (hqca), 92.76, 92.44 (=CH, cod), 30.08, 29.96, 26.39, 26.35, 26.18, 26.12 ($>CH_2$, coe). IR (ATR, cm^{-1}): ν (CO) 1674 (s).

[IrH(κ^3 -hqca)(py)] (6). A resealable Schlenk tube equipped with a Teflon screw valve was charged with [IrH(κ^3 -hqca)(coe)] (3; 0.490 g, 1.00 mmol), pyridine (3 mL), and THF (50 mL). The mixture was heated at 75 °C for 12 h to give a dark red solution. After removal of volatiles, the resulting red solid was dissolved in the minimum amount of CH₂Cl₂ (6 mL). Then, *n*-pentane (25 mL) was slowly added and the resulting mixture kept at low temperature to afford a red solid, which was filtered, washed with *n*-pentane, and dried in vacuo. Yield: 93% (0.500 g). Anal. Calcd for $C_{22}H_{16}IrN_3O_3$: C, 44.60; H, 2.99; N, 7.80. Found: C, 44.79; H, 2.76; N, 7.61. MS (MALDI, CH₂Cl₂, m/z): 617.2 $[M + py]^+$. MS (ESI, CH₂Cl₂, m/z): 617.1 $[M + py]^+$, 461.1 $[M - py]^+$. 1H NMR (400.162 MHz, 298 K, CD₂Cl₂): δ 8.86 (dd, 2H, J_{H-H} = 6.6, 1.4 Hz, *cis*-py), 8.50–8.47 (m, 2H, *trans*-py), 7.82 (d, 1H, J_{H-H} = 8.8 Hz, H-4, hqca), 7.78 (tt, 1H, J_{H-H} = 7.3, 1.4 Hz, *cis*-py), 7.60 (t, 1H, J_{H-H} = 7.3, 1.4 Hz, *trans*-py), 7.47 (d, 1H, J_{H-H} = 8.8 Hz, H-3), 7.31 (t, 1H, J_{H-H} = 8.0 Hz, H-6) (hqca), 7.27 (t, 2H, J_{H-H} = 7.3 Hz, *cis*-py), 7.20 (t, 2H, J_{H-H} = 7.3 Hz, *trans*-py), 6.81 (d, 1H, J_{H-H} = 8.0 Hz, H-5), 6.79 (d, 1H, J_{H-H} = 8.0 Hz, H-7) (hqca), –23.31 (s, 1H, Ir–H). $^{13}C\{^1H\}$ NMR (75.468 MHz, 298 K, CD₂Cl₂): δ 177.04 (C=O), 173.33 (C-8) (hqca), 153.96, 153.91 (*cis*-py), 148.51, 148.41 (*trans*-py), 146.43 (C-2), 145.77 (C-9) (hqca), 137.68 (*trans*-py), 137.04 (*cis*-py), 134.09 (C-6, hqca), 132.36 (2C, *cis*-py), 131.46 (C-10), 125.73 (C-4), (both s, hqca), 125.60 (2C, *trans*-py), 120.73 (C-3), 114.96 (C-5), 112.61 (C-7) (hqca). IR (ATR, cm^{-1}): ν (Ir–H) 2140 (s); ν (CO) 1651 (s).

[IrH(κ^3 -hqca)(2-Mepy)] (7). To a solution of [IrH(κ^3 -hqca)(coe)] (3; 0.245 g, 0.500 mmol) in THF (40 mL) was added 2-methylpyridine (2 mL). Stirring at room temperature for 14 h afforded a red solution. After removal of volatiles under reduced pressure, the resulting red solid was dissolved in the minimum volume of dichloromethane (10 mL). Addition of pentane (30 mL) led to the precipitation of a red-orange solid, which was filtered, washed with pentane (3 \times 10 mL), and dried in vacuo. Yield: 94% (0.266 g). Anal. Calcd for $C_{22}H_{20}IrN_3O_3$: C, 44.63; H, 3.56; N, 7.42. Found: C, 44.79; H, 3.76; N, 7.61. MS (MALDI, CH₂Cl₂, m/z): 474.9 $[M^+ - 2-Mepy]$. MS (ESI, CH₃CN, m/z): 659.2 $[M + 2-Mepy]^+$, 475.1 $[M - 2-Mepy]^+$. 1H NMR (400.162 MHz, 298 K, CD₂Cl₂): δ 8.47 (d, 1H, J_{H-H} = 5.8 Hz, *cis*-2-Mepy), 8.00 (d, 1H, J_{H-H} = 5.1 Hz, *trans*-2-Mepy), 7.91 (d, 1H, J_{H-H} = 8.8 Hz, H-4, hqca), 7.68 (td, 1H, J_{H-H} = 7.3, 1.5 Hz, *cis*-2-Mepy), 7.53 (d, 1H, J_{H-H} = 8.80 Hz, H-3, hqca), 7.52 (td, 1H, J_{H-H} = 7.7, 1.5 Hz, *trans*-2-Mepy), 7.40 (d, 1H, J_{H-H} = 5.1 Hz, *cis*-2-Mepy), 7.37 (t, 1H, J_{H-H} = 8.1 Hz, H-6, hqca), 7.07 (d, 1H, J_{H-H} = 8.0 Hz, *trans*-2-Mepy), 6.99 (t, 1H, J_{H-H} = 6.6 Hz, *cis*-2-Mepy), 6.95 (t, 1H, J_{H-H} = 6.6 Hz, *trans*-2-Mepy), 6.89 (d, 1H, J_{H-H} = 8.1 Hz, H-5), 6.79 (d, 1H, J_{H-H} = 8.0 Hz, H-7) (hqca), 2.81 (s, 3H, –CH₃, *cis*-2-Mepy), 2.12 (s, 3H, –CH₃, *trans*-2-Mepy), –26.06 (s, 1H, Ir–H). $^{13}C\{^1H\}$ NMR (75.468 MHz, 298 K, CD₂Cl₂): δ 172.88 (C=O), 165.89 (C-8), 162.30 (C-2) (hqca), 154.96 (*cis*-2-Mepy), 148.30

(*trans*-2-Mepy), 147.18 (*cis*-2-Mepy), 145.88 (*trans*-2-Mepy), 137.59 (*trans*-2-Mepy), 137.21 (*cis*-2-Mepy), 133.82 (C-6), 132.00 (C-4), 131.34 (C-9 and C-10) (hqca), 126.62 (*trans*-2-Mepy), 125.60 (*cis*-2-Mepy), 122.45 (*cis*-2-Mepy), 122.32 (C-3, hqca), 120.49 (*trans*-2-Mepy), 114.80 (C-7), 112.66 (C-5) (hqca), 26.32 ($-\text{CH}_3$, *cis*-2-Mepy), 22.60 ($-\text{CH}_3$, *trans*-2-Mepy). IR (ATR, cm^{-1}): ν (Ir–H) 2153 (s); ν (CO) 1648 (s).

$[\text{Ir}(\kappa^3\text{-hqca})(1-\kappa\text{-C}_8\text{H}_{15})(\text{CO})(\text{py})]$ (**8**). Carbon monoxide was bubbled through a solution of $[\text{IrH}(\kappa^3\text{-hqca})(\text{coe})(\text{py})]$ (**4**; 0.057 g, 0.1 mmol) in CD_2Cl_2 (2 mL) at room temperature for 1 h 30 min to give a red-orange solution. This solution was transferred into a NMR tube for measurement at low temperature. ^1H NMR (300.13 MHz, 233 K, CD_2Cl_2): δ 8.55 (dd, 2H, $J_{\text{H-H}} = 6.3$, 1.4 Hz, o-H, py), 8.34 (d, 1H, $J_{\text{H-H}} = 8.7$ Hz, H-4), 7.84 (d, 1H, $J_{\text{H-H}} = 8.7$ Hz, H-3), (hqca), 7.79 (tt, 1H, $J_{\text{H-H}} = 7.7$, 1.4 Hz, p-H, py), 7.56 (t, 1H, $J_{\text{H-H}} = 8.1$ Hz, H-6, hqca), 7.38 (t, 2H, $J_{\text{H-H}} = 7.0$ Hz, m-H, py), 7.08 (d, 1H, $J_{\text{H-H}} = 7.2$ Hz, H-5), 7.06 (d, 1H, $J_{\text{H-H}} = 7.4$ Hz, H-7) (hqca), 1.80–1.10 (set of m, 15H, $\kappa\text{-C}_8\text{H}_{15}$). $^{13}\text{C}\{^1\text{H}\}$ NMR (75.468 MHz, 233 K, CD_2Cl_2): δ 173.83 (C=O, hqca), 171.56 (CO), 169.17 (C-8, hqca), 149.27 (2C, py), 143.03 (C-2), 140.87 (C-9) (hqca), 138.83 (py), 138.57 (C-6), 133.83 (C-4), 131.79 (C-10) (hqca), 126.05 (2C, py), 121.43 (C-3), 116.01 (C-7), 113.36 (C-5) (hqca), 36.53, 35.79, 27.53, 27.49, 27.31, 26.92, 26.11 ($>\text{CH}_2$), 21.61 (Ir–CH) ($\kappa\text{-C}_8\text{H}_{15}$). IR (CH_2Cl_2 , cm^{-1}): ν (CO) 2031 (s), 1675 (s).

General Procedure for the Catalytic Borylation Reactions.

The catalytic borylation of aromatic compounds was carried out under an argon atmosphere in a glass reaction tube fitted with a greaseless high-vacuum stopcock (Kontes tube). The reactions were conducted in the aromatic substrate as solvent using HBpin or B_2pin_2 as the boron source with iridium catalyst loadings of 2.5 mol % (for HBpin) or 5.0 mol % (for B_2pin_2) in order to maintain the boron/iridium ratio. In a typical experiment, the reactor was charged with the catalyst (0.0037 mmol), the corresponding arene (22 mmol), and HBpin (21.2 μL , 0.146 mmol) or B_2pin_2 (18.62 mg, 0.073 mmol) and the solution stirred and heated at the required temperature for 20 h. The solvent was removed under vacuum at room temperature and the residue analyzed by ^1H NMR in order to determine the conversion and selectivity. Identification of the products was done by comparison of the spectroscopic data with those reported in the literature.

DOSY Experiments. ^1H DOSY (diffusion-ordered spectroscopy) NMR experiments were performed on a Bruker Avance 400 MHz spectrometer.⁴³ Solutions of $[\text{IrH}(\kappa^3\text{-hqca})(\text{coe})]$ (**3**; 10 mg, 0.020 mmol, in 0.5 mL of deuterated solvent, 4.0×10^{-2} M) in tetrahydrofuran- d_8 and benzene- d_6 were prepared using the same batch sample. The experiments were acquired with the pulse program steppg1s (Bruker software) at 300 K with spinning of the sample to avoid convection influence (air flow of 400 L h^{-1}). The diffusion coefficients (D) were determined from the measurements of the progressive decay of the intensities of selected resonances, aromatic peaks or hydride resonances, with an increase in the gradient strength. The raw data were processed using the Bruker DOSY package and T1/T2 relaxation module, which directly provided the D values. The fitting curves for both sets of DOSY experiments are available in the Supporting Information. The hydrodynamic radii were calculated by applying a modified Stokes–Einstein equation.⁴⁴

Theoretical Calculations. The computational studies were carried out using the Gaussian09 package.⁴⁵ Molecular structures were optimized using the B3LYP functional and lanl2dz effective core potential for iridium along the lanl2dz basis set augmented with an f type polarization function.⁴⁶ For the rest of the atoms the built-in 6-31G** basis set was used. The minima found were confirmed by frequency analysis. The natural charges on the hydride ligands were calculated with the NBO 5.0 program.³⁵ The structures of the optimized molecules were depicted with the CyIview program.⁴⁷ Molecular volume calculations were carried out by a series of 15 Monte Carlo integrated volume calculations with the Volume keyword and tight option in Gaussian09, which takes the molecular volume inside a contour of density 0.001 electron/bohr³. The reported radii were those recommended by Gaussian to be used as cavity radii in solvent calculations. These radii are 0.5 Å larger than the radii

corresponding to the calculated volume above, in order to allow for the solvent-excluded volume.⁴⁵

Crystal Structure Determinations of $[\text{Ir}(\kappa^3\text{-hqca})(1-\kappa\text{-4,5-}\eta\text{-C}_8\text{H}_{13})]$ (1a**) and $[\text{IrH}(\kappa^3\text{-hqca})(\text{py})_2]$ (**6**).** Single crystals for the X-ray diffraction study of **1a** (red prisms) were grown by slow diffusion of diethyl ether into a $\text{CH}_2\text{Cl}_2/\text{MeOH}$ solution of the compound at 258 K. Crystals of **6** (red prisms) were obtained by slow diffusion of *n*-hexane into a tetrahydrofuran solution at 243 K. X-ray diffraction data were collected at 100(2) K on a Bruker SMART APEX CCD area detector diffractometer with graphite-monochromated Mo $K\alpha$ radiation ($\lambda = 0.71073$ Å) using narrow ω rotations (0.3°). Intensities were integrated with the SAINT-PLUS program⁴⁸ and corrected for absorption effects with SADABS.⁴⁹ The structures were solved by Patterson methods with SHELXS-97.⁵⁰ Refinements, by full-matrix least squares on F^2 with SHELXL-97,⁵¹ were similar for both complexes, including isotropic and subsequently anisotropic displacement parameters of non-H nondisordered atoms. Hydrogen atoms for both molecules were included from observed positions and refined with displacement riding parameters. All of the observed residuals over 1 $\text{e}/\text{\AA}^3$ in the final Fourier maps were in close proximity of the metal center, having no chemical sense.

Crystal data for **1a:** $\text{C}_{19}\text{H}_{22}\text{IrNO}_4 \cdot 2\text{CH}_2\text{Cl}_2$, $M_r = 690.43$; red irregular block, $0.211 \times 0.203 \times 0.152$ mm³; triclinic, $P\bar{1}$; $a = 10.0950(7)$ Å, $b = 11.0369(8)$ Å, $c = 12.0268(9)$ Å, $\alpha = 98.1630(10)^\circ$, $\beta = 113.8100(10)^\circ$, $\gamma = 100.9380(10)^\circ$; $Z = 2$; $V = 1167.49(15)$ Å³; $D_c = 1.964$ g/cm³; $\mu = 6.205$ mm^{−1}, minimum and maximum absorption correction factors 0.356 and 0.456; $2\theta_{\text{max}} = 54.08^\circ$; 13820 reflections collected, 5070 unique reflections ($R_{\text{int}} = 0.0278$); 5070/0/360 data/restraints/parameters; final GOF 1.103; $R_1 = 0.0257$ (4836 reflections, $I > 2\sigma(I)$), $wR_2 = 0.0641$ for all data; largest difference peak 3.44 $\text{e}/\text{\AA}^3$. Two dichloromethane solvent molecules were present in the asymmetric unit.

Crystal data for **6:** $\text{C}_{20}\text{H}_{16}\text{IrN}_3\text{O}_3 \cdot \text{H}_2\text{O}$, $M_r = 556.60$; red prism, $0.073 \times 0.065 \times 0.045$ mm³; monoclinic, $P2_1/n$; $a = 8.3967(9)$ Å, $b = 15.3084(17)$ Å, $c = 14.1731(16)$ Å, $\beta = 90.6360(10)^\circ$; $Z = 4$; $V = 1821.7(3)$ Å³; $D_c = 2.029$ g/cm³; $\mu = 7.362$ mm^{−1}, minimum and maximum absorption correction factors 0.626 and 0.720; $2\theta_{\text{max}} = 55.74^\circ$; 20909 reflections collected, 4241 unique reflections ($R_{\text{int}} = 0.0606$); 4241/1/310 data/restraints/parameters; final GOF 1.113; $R_1 = 0.0396$ (3397 reflections, $I > 2\sigma(I)$), $wR_2 = 0.0819$ for all data; largest difference peak 2.693 $\text{e}/\text{\AA}^3$. A water molecule was also present in the crystal structure. A geometrical restraint in the Ir–H distance was included in the refinement.

■ ASSOCIATED CONTENT

§ Supporting Information

CIF files giving X-ray crystallographic data for the structure determination of compounds **1a** and **6** and text, tables, and figures giving experimental details on the ^1H DOSY NMR experiments, optimized coordinates and van der Waals surface for the model compounds, and calculated energies for the determination of ΔG° for the formation of the species **3–L**. This material is available free of charge via the Internet at <http://pubs.acs.org>.

■ AUTHOR INFORMATION

Corresponding Authors

*J.J.P.-T.: tel, 34 976762025; fax, 34 976761143; perez@unizar.es.

*L.A.O.: e-mail, oro@unizar.es.

Notes

The authors declare no competing financial interest.

■ ACKNOWLEDGMENTS

Financial support from the Ministerio de Economía y Competitividad (MEC/FEDER) of Spain (Project CTQ2010-15221), Diputación General de Aragón (Group E07) and

Fondo Social Europeo, and CONSOLIDER INGENIO-2010, under the Projects MULTICAT (CSD2009-00050) and Factoría de Crystalización (CSD2006-0015), is gratefully acknowledged.

REFERENCES

- (1) (a) *The Chemistry of Pincer Compounds*; Morales-Morales, D., Jensen, C. M., Eds.; Elsevier: Amsterdam, 2007. (b) *Organometallic Pincer Chemistry*; van Koten, G., Milstein, D., Eds.; Springer-Verlag: Berlin, 2013; Topics in Organometallic Chemistry 40.
- (2) (a) Peris, E.; Crabtree, R. H. *Coord. Chem. Rev.* **2004**, *248*, 2239–2246. (b) van der Boom, M. E.; Milstein, D. *Chem. Rev.* **2003**, *103*, 1759–1792.
- (3) (a) Zhang, G.; Scott, B. L.; Hanson, S. K. *Angew. Chem., Int. Ed.* **2012**, *51*, 12102–12106. (b) Sun, Y.; Koehler, C.; Tan, R.; Annibale, V. T.; Song, D. *Chem. Commun.* **2011**, *47*, 8349–8351. (c) Huff, C. A.; Sanford, M. S. *J. Am. Chem. Soc.* **2011**, *133*, 18122–18125. (d) Zhang, J.; Leitus, G.; Ben-David, Y.; Milstein, D. *Angew. Chem., Int. Ed.* **2006**, *45*, 1113–1115.
- (4) (a) HaiBach, M. C.; Kundu, S.; Brookhart, M.; Goldman, A. S. *Acc. Chem. Res.* **2012**, *45*, 947–958. (b) Ahuja, R.; Punji, B.; Findlater, M.; Supplee, C.; Schinki, W.; Brookhart, M.; Golman, A. S. *Nat. Chem.* **2011**, *3*, 167–171. (c) Choi, J.; MacArthur, A. H. R.; Brookhart, M.; Goldman, A. S. *Chem. Rev.* **2011**, *111*, 1761–1779.
- (5) (a) Selander, N.; Szabó, K. J. *Chem. Rev.* **2011**, *111*, 2048–2076. (b) Benito-Garagorri, D.; Kircher, K. *Acc. Chem. Res.* **2008**, *41*, 201–213.
- (6) (a) McLaughlin, M. P.; Adduci, L. L.; Becker, J. J.; Gagné, M. R. *J. Am. Chem. Soc.* **2013**, *135*, 1225–1227. (b) Arai, T.; Oka, I.; Morihata, T.; Awata, A.; Masu, H. *Chem. Eur. J.* **2013**, *19*, 1554–1557. (c) Lee, C. I.; Zhou, J.; Ozerov, O. V. *J. Am. Chem. Soc.* **2013**, *135*, 3560–3566. (d) Park, S.; Bézier, D.; Brookhart, M. *J. Am. Chem. Soc.* **2012**, *134*, 11404–11407. (e) Gunanathan, C.; Milstein, D. *Acc. Chem. Res.* **2011**, *44*, 588–602. (f) Choi, J.; Wang, D. Y.; Kundu, S.; Choliy, Y.; Emge, T. J.; Krogh-Jespersen, K.; Golman, A. S. *Science* **2011**, *332*, 1545–1548. (g) Gossage, R. A.; van De Kuil, L. A.; van Koten, G. *Acc. Chem. Res.* **1998**, *31*, 423–431.
- (7) Goldman, A. S.; Roy, A. H.; Huang, Z.; Ahuja, R.; Schinski, W.; Brookhart, M. *Science* **2006**, *312*, 257–261.
- (8) (a) Arduengo, A. J.; Dolphin, J. S.; Gurău, G.; Marshall, W. J.; Nelson, J. C.; Petrov, V. A.; Runyon, J. W. *Angew. Chem., Int. Ed. Engl.* **2013**, *52*, 5110. (b) Romain, C.; Brelot, L.; Bellemín-Lapponnaz, S.; Dagorne, S. *Organometallics* **2010**, *29*, 1191–1198. (c) Klein, A.; Elmas, S.; Butsch, K. *Eur. J. Inorg. Chem.* **2009**, 2271–2281. (d) Agapie, T.; Day, M. W.; Bercaw, J. E. *Organometallics* **2008**, *27*, 6123–6142. (e) Agapie, T.; Henling, L. H.; DiPasquale, A. G.; Rheingold, A. L.; Bercaw, J. E. *Organometallics* **2008**, *27*, 6245–6256.
- (9) (a) O'Reilly, M. E.; Ghiviriga, I.; Abboud, K. A.; Veige, A. S. *J. Am. Chem. Soc.* **2012**, *134*, 11185–11195. (b) Sarkar, S.; McGowan, K. P.; Kuppuswamy, S.; Ghiviriga, I.; Abboud, K. A.; Veige, A. S. *J. Am. Chem. Soc.* **2012**, *134*, 4509–4512. (c) O'Reilly, M. E.; Del Castillo, T. J.; Abboud, K. A.; Veige, A. S. *Dalton Trans.* **2012**, *41*, 2237–2246. (d) Kuppuswamy, S.; Peloquin, A. J.; Ghiviriga, I.; Abboud, K. A.; Veige, A. S. *Organometallics* **2010**, *29*, 4227–4233.
- (10) (a) Szigethy, G.; Heyduk, A. F. *Dalton Trans.* **2012**, *41*, 8144–8152. (b) Lu, F.; Zarkesh, R. A.; Heyduk, A. F. *Eur. J. Inorg. Chem.* **2012**, 467–470. (c) Heyduk, A. F.; Zarkesh, R. A.; Nguyen, A. I. *Inorg. Chem.* **2011**, *50*, 9849–9863. (d) Zarkesh, R. A.; Heyduk, A. F. *Organometallics* **2011**, *30*, 4890–4898.
- (11) (a) *Activation and Functionalization of C-H Bonds*; Goldberg, K. I.; Goldman, A. S., Eds.; American Chemical Society: Washington, DC, 2004; ACS Symposium Series 885. (b) Simmons, E. M.; Hartwig, J. F. *Nature* **2012**, *483*, 70–73. (c) Crabtree, R. H. *Chem. Rev.* **2010**, *110*, 575–575.
- (12) (a) Hartwig, J. F. *Acc. Chem. Res.* **2012**, *45*, 864–873. (b) Mkhali, I. A. I.; Barnard, J. H.; Marder, T. B.; Murphy, J. M.; Hartwig, J. F. *Chem. Rev.* **2010**, *110*, 890–931. (c) Arndtsen, B. A.; Bergman, R. G.; Mobley, T. A.; Peterson, T. H. *Acc. Chem. Res.* **1995**, *28*, 154–162.
- (13) (a) Fu, R.; Bercaw, J. E.; Labinger, J. A. *Organometallics* **2011**, *30*, 6751–6765. (b) Weinberg, D. R.; Hazari, N.; Labinger, J. A.; Bercaw, J. E. *Organometallics* **2010**, *29*, 89–100.
- (14) (a) Hashiguchi, B. G.; Bischof, S. M.; Konnick, M. M.; Periana, R. A. *Acc. Chem. Res.* **2012**, *45*, 886–898. (b) Bhalla, G.; Lui, X. Y.; Oxgaard, J.; Goddard, W. A.; Periana, R. A. *J. Am. Chem. Soc.* **2005**, *127*, 11372–11389.
- (15) Nguyen, D. H.; Pérez-Torrente, J. J.; Lomba, L.; Jiménez, M. V.; Lahoz, F. J.; Oro, L. A. *Dalton Trans.* **2011**, *40*, 8429–8435.
- (16) Nguyen, D. H.; Greger, I.; Pérez-Torrente, J. J.; Jiménez, M. V.; Modrego, F. J.; Lahoz, F. J.; Oro, L. A. *Organometallics* **2013**, DOI: 10.1021/om400767d.
- (17) (a) Tong, L.; Wang, Y.; Duan, L.; Xu, Y.; Cheng, X.; Fischer, A.; Ahlquist, M. S. G.; Sun, L. *Inorg. Chem.* **2012**, *51*, 3388–3398. (b) Hanson, S. K.; Baker, R. T.; Gordon, J. C.; Scott, B. L.; Silks, L. A.; Thorn, D. L. *J. Am. Chem. Soc.* **2010**, *132*, 17804–17816.
- (18) Albert, A.; Phillips, J. N. *J. Chem. Soc.* **1956**, 1294–1304.
- (19) Armarego, W. L. F.; Chai, C. L. L. *Purification of Laboratory Chemicals*; Elsevier: Amsterdam, 2003; p 346.
- (20) Bombi, G. G.; Aikebaier, R.; Dean, A.; Di Marco, V. B.; Marton, D.; Tapparo, A. *Polyhedron* **2009**, *28*, 327–335.
- (21) (a) Acharyya, R.; Basuli, F.; Peng, S. M.; Lee, G. H.; Wang, R. Z.; Mak, T. C. W.; Bhattacharya, S. J. *Organomet. Chem.* **2005**, *690*, 3908–3917. (b) Acharyya, R.; Basuli, F.; Wang, R. Z.; Mak, T. C. W.; Bhattacharya, S. *Inorg. Chem.* **2004**, *43*, 704–711. (c) Ladipo, F. T.; Kooti, M.; Merola, J. S. *Inorg. Chem.* **1993**, *32*, 1681–1688.
- (22) (a) Di Giuseppe, A.; Castarlenas, R.; Pérez-Torrente, J. J.; Lahoz, F. J.; Polo, V.; Oro, L. A. *Angew. Chem., Int. Ed.* **2011**, *50*, 3938–3942. (b) Findlater, M.; Cartwright-Sykes, A.; White, P.; Schauer, C. K.; Brookhart, M. *J. Am. Chem. Soc.* **2011**, *133*, 12274–12284. (c) Burling, S.; Haller, L. J. L.; Mas-Marza, E.; Moreno, A.; Macgregor, S. A.; Mahon, M. F.; Pregosin, P. S.; Whittlesey, M. K. *Chem. Eur. J.* **2009**, *15*, 10912–10923. (d) Ben-Ari, E.; Gandelman, M.; Rozenberg, H.; Shimon, L. J. W.; Milstein, D. *J. Am. Chem. Soc.* **2003**, *125*, 4714–4715.
- (23) *Nomenclature of Inorganic Chemistry. IUPAC Recommendations 2005*; Connolly, N. G.; Damhus, T., Eds.; Royal Society of Chemistry: Cambridge, U.K., 2005.
- (24) Sakaki, S.; Takayama, T.; Sumimoto, M.; Sugimoto, M. *J. Am. Chem. Soc.* **2004**, *126*, 3332–3348.
- (25) Morris, G. A. Diffusion-Ordered Spectroscopy. In *Encyclopedia of Magnetic Resonance*; Harris, R. K.; Wasylishen, R. E., Eds.; Wiley: Chichester, U.K., 2009.
- (26) Chen, H.-C.; Chen, S.-H. *J. Phys. Chem.* **1984**, *88*, 5118–5121.
- (27) Stereochemistry of the possible *cis* assemblies: μ -bis-carboxylato, CC/AA (C_2); μ -bis-alkoxo, CC/AA (C_2); μ -carboxylato-alkoxo, CA/AC (C_1).
- (28) Nakamoto, K. *Infrared and Raman Spectra of Inorganic and Coordination Compounds: Applications in Coordination, Organometallic, and Bioinorganic Chemistry*; Wiley-Interscience: New York, 1997.
- (29) (a) Das, B.; Baruah, J. B. *Polyhedron* **2012**, *31*, 361–367. (b) Hu, J.; Li, J.; Zhao, J.; Hou, H.; Fan, Y. *Inorg. Chim. Acta* **2009**, *362*, 5023–5030.
- (30) (a) Acha, F.; Garralda, M. A.; Ibarlucea, L.; Pinilla, E.; Torres, M. R. *Inorg. Chem.* **2005**, *44*, 9084–9091. (b) Chin, C. S.; Yoon, J.; Song, J. *Inorg. Chem.* **1993**, *32*, 5901–5904.
- (31) Olgemöller, B.; Beck, W. *Inorg. Chem.* **1983**, *22*, 997–998.
- (32) Gutmann, V. *Coord. Chem. Rev.* **1976**, *18*, 225–255.
- (33) (a) Atkinson, K. D.; Cowley, M. J.; Elliott, P. I. P.; Duckett, S. B.; Green, G. G. R.; Lopez-Serrano, J.; Whitwood, A. C. *J. Am. Chem. Soc.* **2009**, *131*, 13362–13368. (b) Atkinson, K. D.; Cowley, M. J.; Duckett, S. B.; Elliott, P. I. P.; Green, G. G. R.; Lopez-Serrano, J.; Khazal, I. G.; Whitwood, A. C. *Inorg. Chem.* **2009**, *48*, 663–670.
- (34) Dedieu, A. *Transition Metal Hydrides: Recent Advances in Theory and Experiment*; VCH: New York, 1991.
- (35) Glendening, E. D.; Badenhop, J. K.; Reed, A. E.; Carpenter, J. E.; Bohmann, J. A.; Morales, C. M.; Weinhold, F. *NBO 5.0*;

Theoretical Chemistry Institute, University of Wisconsin, Madison, WI, 2001.

(36) (a) Ito, J.; Kaneda, T.; Nishiyama, H. *Organometallics* **2012**, *31*, 4442–4449. (b) Chianese, A. R.; Mo, A.; Lampland, N. L.; Swartz, R. L.; Bremer, P. T. *Organometallics* **2010**, *29*, 3019–3026.

(37) Yinghuai, Z.; Yan, K. C.; Jizhong, L.; Hwei, C. S.; Hon, Y. C.; Emi, A.; Zhenshun, S.; Winata, M.; Hosmane, N. S.; Maguire, J. A. *J. Organomet. Chem.* **2007**, *692*, 4244–4250.

(38) Ishiyama, T.; Takagi, J.; Ishida, K.; Miyaura, N.; Anastasi, N. R.; Hartwig, J. F. *J. Am. Chem. Soc.* **2002**, *124*, 390–391.

(39) Dang, L.; Lin, Z.; Marder, T. B. *Chem. Commun.* **2009**, 3987–3995.

(40) (a) Boller, T. M.; Murphy, J. M.; Hapke, M.; Ishiyama, T.; Miyaura, N.; Hartwig, J. F. *J. Am. Chem. Soc.* **2005**, *127*, 14263–14278.

(b) Tamura, H.; Yamazaki, H.; Sato, H.; Sakaki, S. *J. Am. Chem. Soc.* **2003**, *125*, 16114–16126.

(41) Uson, R.; Oro, L. A.; Cabeza, J. A. *Inorg. Synth.* **1985**, *23*, 126–130.

(42) Ortmann, D. A.; Werner, H. Z. *Anorg. Allg. Chem.* **2002**, *628*, 1373–1376.

(43) For recent reviews on NMR diffusion methods see: (a) Pregosin, P. S. *Prog. Nucl. Magn. Reson. Spectrosc.* **2006**, *49*, 261–288. (b) Cohen, Y.; Avram, L.; Frish, L. *Angew. Chem., Int. Ed.* **2005**, *44*, 520–554. (c) Brand, T. E.; Cabrita, J.; Berger, S. *Prog. Nucl. Magn. Reson. Spectrosc.* **2005**, *46*, 159–196. (d) Pregosin, P. S.; Kumar, P. G. A.; Fernandez, I. *Chem. Rev.* **2005**, *105*, 2977–2998.

(44) (a) Krempner, C.; Chisholm, M. H.; Gallucci, J. *Angew. Chem., Int. Ed.* **2008**, *47*, 410–413. (b) Zuccaccia, C. N.; Stahl, G.; Macchioni, A.; Chen, M.-C.; Roberts, J. A.; Marks, T. J. *J. Am. Chem. Soc.* **2004**, *126*, 1448–1464. (c) Zuccaccia, D.; Sabatini, S.; Bellachioma, G.; Cardaci, G.; Clot, E.; Macchioni, A. *Inorg. Chem.* **2003**, *42*, 5465–5467 and references therein.

(45) Frisch, M. J.; Trucks, G. W.; Schlegel, H. B.; Scuseria, G. E.; Robb, M. A.; Cheeseman, J. R.; Scalmani, G.; Barone, V.; Mennucci, B.; Petersson, G. A.; Nakatsuji, H.; Caricato, M.; Li, X.; Hratchian, H. P.; Izmaylov, A. F.; Bloino, J.; Zheng, G.; Sonnenberg, J. L.; Hada, M.; Ehara, M.; Toyota, K.; Fukuda, R.; Hasegawa, J.; Ishida, M.; Nakajima, T.; Honda, Y.; Kitao, O.; Nakai, H.; Vreven, T.; Montgomery, J. A.; Peralta, J. E.; Ogliaro, F.; Bearpark, M.; Heyd, J. J.; Brothers, E.; Kudin, K. N.; Staroverov, V. N.; Kobayashi, R.; Normand, J.; Raghavachari, K.; Rendell, A.; Burant, J. C.; Iyengar, S. S.; Tomasi, J.; Cossi, M.; Rega, N.; Millam, J. M.; Klene, M.; Knox, J. E.; Cross, J. B.; Bakken, V.; Adamo, C.; Jaramillo, J.; Gomperts, R.; Stratmann, R. E.; Yazyev, O.; Austin, A. J.; Cammi, R.; Pomelli, C.; Ochterski, J. W.; Martin, R. L.; Morokuma, K.; Zakrzewski, V. G.; Voth, G. A.; Salvador, P.; Dannenberg, J. J.; Dapprich, S.; Daniels, A. D.; Farkas, Foresman, J. B.; Ortiz, J. V.; Cioslowski, J.; Fox, D. J. *Gaussian 09, Revision B.01*; Gaussian Inc., Wallingford, CT, 2009.

(46) Ehlers, A.; Böhme, M.; Dapprich, S.; Gobbi, A.; Höllwarth, A.; Jonas, V.; Köhler, K.; Stegmann, R.; Veldkamp, A.; Frenking, G. *Chem. Phys. Lett.* **1993**, *208*, 111–114.

(47) Legault, C. Y. *CYLview*; Université de Sherbrooke, Sherbrooke, Canada, 2009.

(48) SAINT-PLUS, version 6.01; Bruker AXS, Inc., Madison, WI, USA, 2001.

(49) Sheldrick, G. M. *SADABS*; University of Göttingen, Göttingen, Germany, 1999.

(50) (a) Sheldrick, G. M. *Methods Enzymol.* **1997**, *276*, 628–641.

(b) Sheldrick, G. M. *Acta Crystallogr.* **1990**, *A46*, 467–473.

(51) Sheldrick, G. M. *Acta Crystallogr.* **2008**, *A64*, 112–122.